12

Modeling Stochastic Volatility

This chapter introduces into the pricing and hedging of derivatives under stochastic volatility. The emphasis is on standard derivatives for various index models. We choose as underlying security a diversified index, which we interpret as GOP.

12.1 Stochastic Volatility

Stochastic Volatility of an Index

Since a diversified accumulation index can be interpreted as a diversified portfolio we assume that its dynamics are closely approximated by that of a GOP. The value $S_t^{\delta_*}$ of a GOP at time t satisfies by (10.2.8) the SDE

$$dS_t^{\delta_*} = S_t^{\delta_*} \left(r_t \, dt + |\theta_t| \, (|\theta_t| \, dt + dW_t) \right) \tag{12.1.1}$$

for $t \in [0, \infty)$ with $S_0^{\delta_*} > 0$. Here $r = \{r_t, \, t \in [0, \infty)\}$ is the short term interest rate process, which we assume in this chapter, for simplicity, to be constant, such that $r_t = r \geq 0$ for all $t \in [0, \infty)$. Furthermore, $|\theta_t|$ denotes the volatility of the GOP at time t, which is the, in general, stochastic total market price of risk, see (11.1.11). Finally, $W = \{W_t, \, t \in [0, \infty)\}$ is a standard Wiener process on $(\Omega, \mathcal{A}, \underline{\mathcal{A}}, P)$. Note that the volatility and the short rate characterize the dynamics of the GOP in the denomination of the domestic currency.

If we consider the logarithm of the GOP, then the SDE follows by the Itô formula and (12.1.1) in the form

$$d \ln \left(S_t^{\delta_*} \right) = \left(r + \frac{1}{2} \, |\theta_t|^2 \right) dt + |\theta_t| \, dW_t \tag{12.1.2}$$

for $t \in [0, \infty)$, see Exercise 13.1. This allows us to obtain the GOP volatility $|\theta_t|$ at time t by the volatility formula (5.2.14) as the time derivative of the quadratic variation of $\ln(S_t^{\delta_*})$, that is,

E. Platen, D. Heath, *A Benchmark Approach to Quantitative Finance*,
Springer Finance,

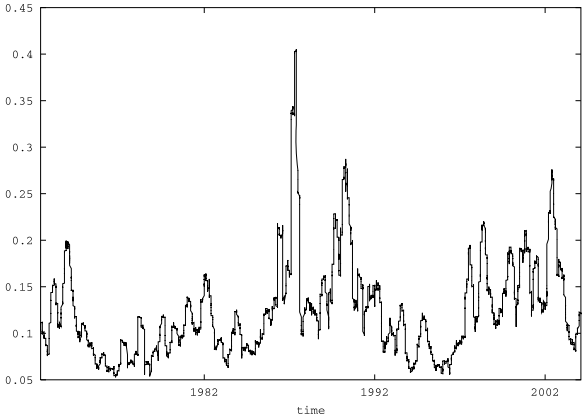

Fig. 12.1.1. Estimated volatility of WSI from 1973–2004

$$|\theta_t| = \sqrt{\frac{d}{dt}\left[\ln\left(S^{\delta_*}\right)\right]_t} \tag{12.1.3}$$

for $t \in [0, \infty)$. In Fig. 12.1.1 we plot for the WSI from Fig. 10.6.5, based on daily observations, the volatility which was obtained numerically by using the formula (12.1.3) for the period from 1973 until 2004. One observes that the volatility of this stock index is not a constant or a simple deterministic function of time. Obviously, it is a stochastic process with clusters of higher values. Taking this into account, the BS model is certainly not a perfect description of reality.

Leverage Effect

To illustrate systematic deviations of an index dynamics from the BS model a study was undertaken by Kelly (1999). Using the standard BS model with constant volatility the P&L, that is the hedge error, was minimized when hedging a European call option with given strike K and given time to maturity T, as described in Chap. 8. By using daily data from 1990 until 1998 from the S&P500 and a fixed volatility for the BS model the resulting average hedge errors are shown in Fig. 12.1.2 with dependence on moneyness. These hedge errors express the average P&L when exhausting all possible periods allowed by the data for the hedge analysis. One notes that there is a strong negative skew in the P&L from hedging European calls under the BS model. This indicates that an improved model for such an index needs to account for this stylized empirical feature, which one can also document for other time periods. Note that in this simple experiment no traded option prices from the market were involved.

The negative skew in Fig. 12.1.2 is a reflection of the *leverage effect*, see Black (1976), which expresses a negative correlation between the index and its volatility. When the index value increases the volatility decreases and vice

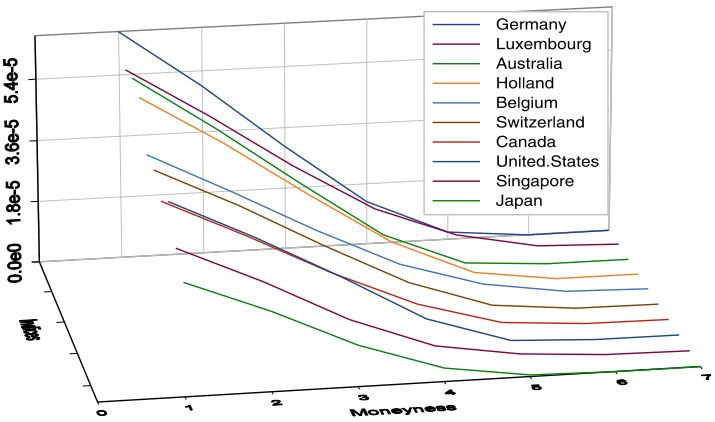

Fig. 12.1.2. Estimated hedge error for S&P500 under BS model

versa. To give an economic interpretation of the leverage effect let us interpret the index as a stock market index. If the index is relatively high, then the average market value of companies is rather high and the debt that these companies have, appears to be comparably low. Such a situation corresponds to low risk, which is reflected in low volatility of the index. On the other hand, there is a much higher risk associated with these companies if the market index is relatively low. For a low stock market index level the debt of the companies appears to be relatively high and the volatility, as a measure of risk, is therefore comparably high. This basic economic relationship explains, in principle, the observed negative correlation between the stock market index and its volatility. The leverage effect has been empirically documented in many ways, for instance, it was studied in Black (1976). It is a challenge for an advanced index model to explain and reflect this effect in a consistent and parsimonious manner, in particular, over long periods of time. A crucial step would be to reveal a potential functional dependence between index and volatility.

Implied Volatilities

Stylized facts on stochastic volatility for traded index options are well documented in the econometrics and finance literature. For example Bollerslev, Chou & Kroner (1992) provide a survey using *autoregressive conditional heteroscedastic* (ARCH) models and Ghysels, Harvey & Renault (1996), Frey (1997) and Cont & Tankov (2004) provide reviews on stochastic volatility models.

In principle, the only parameter in the Black & Scholes (1973) option pricing formula, see (8.3.2), that cannot be directly observed is the volatility. Thus, by using certain given option prices the corresponding *implied volatility* can be

obtained by inverting the Black-Scholes formula (8.3.2), as will be explained below.

There exists a liquid market for European call and put options on most stock indices. One can use the observed market prices to detect deviations from the BS model that traders, who survived successfully in the market, have learned to take into account. Let us denote by

$$c_{T,K}(0, S, \sigma, r) = c_{T,K}(0, S) \tag{12.1.4}$$

the European call option price at time $t = 0$ obtained from the Black-Scholes formula (8.3.2) when the volatility is $\sigma > 0$, the short rate $r \in [0, \infty)$, the time to maturity $T \in [0, \infty)$, the actual value of the underlying index $S > 0$ and the strike price equals $K > 0$. From the traded European call option price $V_{c,T,K}(0, S_0)$ with strike price K and time to maturity T, which is observed in the market for an index with value S_0 at the time $t = 0$, one can deduce the *implied volatility* $\sigma_{\rm BS}^{\rm call}(0, S_0, T, K, r)$ by setting

$$V_{c,T,K}(0, S_0) = c_{T,K}\left(0, S_0, \sigma_{\rm BS}^{\rm call}(0, S_0, T, K, r), r\right). \tag{12.1.5}$$

There is no explicit solution to this equation and one needs to find the implied volatility $\sigma_{\rm BS}^{\rm call}(0, S_0, T, K, r)$ by some root finding method. For instance, the well-known Newton-Raphson iteration method can be used. Similarly, one finds implied volatilities for European puts. One can also price European call or put options according to a given model, for instance the MMM, and calculate the corresponding implied volatilities.

In the market it is often observed that away-from-the-money equity and exchange rate options have higher implied volatilities than at-the-money options. This phenomenon is commonly called the implied volatility *smile*, as for instance discussed in Rubinstein (1985), Clewlow & Xu (1994), Derman & Kani (1994a), Taylor & Xu (1994) or Platen & Schweizer (1998). For indices one observes a *negative skew* in the implied volatilities. This is also consistent with the pattern of hedge errors in Fig. 12.1.2 and is a manifestation of the leverage effect.

For the S&P500 in Fig. 12.1.3 we show implied volatilities for three months to maturity European options for the period from 1997 until 1998 in dependence on the moneyness $\frac{K}{S}$ of the strike over the underlying index value. One notes that the implied volatilities are not the same for different moneyness. Furthermore, one notes that the negatively skewed implied volatility curves evolve over time. In Fig. 12.1.4 we show implied volatilities of one year options, that is, for time to maturity $T = 1$, for the S&P500 during the same period. Note that the curvature of these implied volatility curves is less pronounced than that of the shorter dated options shown in Fig. 12.1.3. This leads to an implied volatility term structure.

More precisely, at a fixed time one can generate an *implied volatility surface* from observed option prices by interpolation over different maturities and strikes. Such a surface reflects the deviations of traded option prices from BS

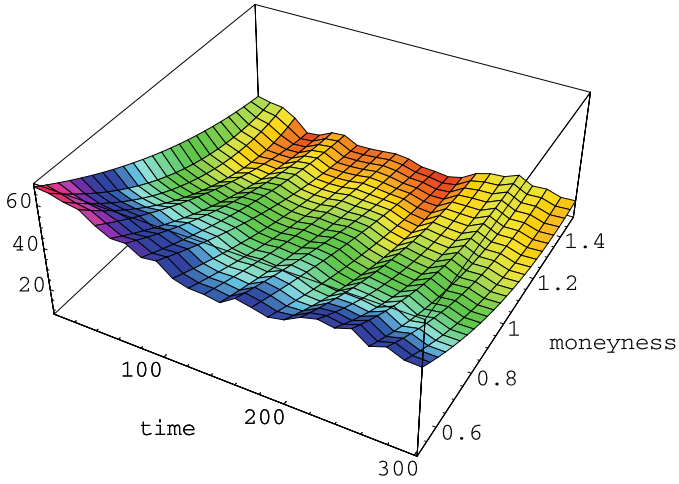

Fig. 12.1.3. Implied volatilities for S&P500 three month options

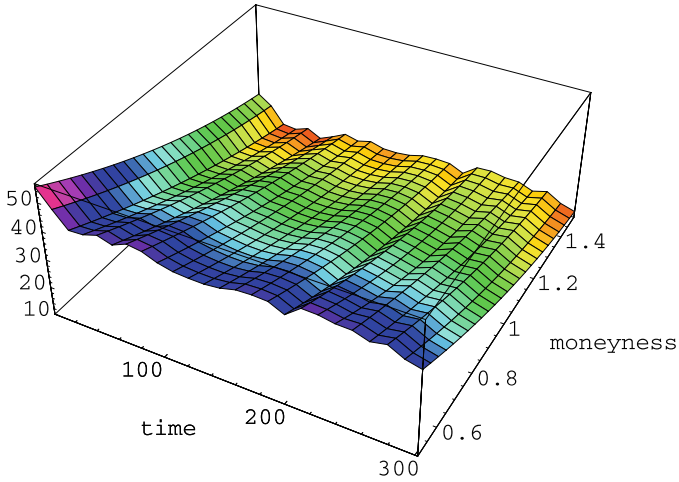

Fig. 12.1.4. Implied volatilities for S&P500 one year options

option prices. In Cont & da Fonseca (2002) an average shape of the implied volatility surface for European options on the S&P500 has been extracted. For the one year period from March 2000 until February 2001 we plot in Fig. 12.1.5 a graph that shows approximately the observed average shape of the implied volatility surface. This surface is negatively skewed with less curvature for larger times to maturity. For shorter times to maturity the implied volatility surface is more curved in a convex manner. At the money, the implied volatility shows a slight systematic increase over time. These stylized empirical facts should be explained by an advanced index model. Additionally, it is also observed that the implied volatility with fixed strike, say at-the-money, and fixed maturity, for instance one month, changes randomly over time.

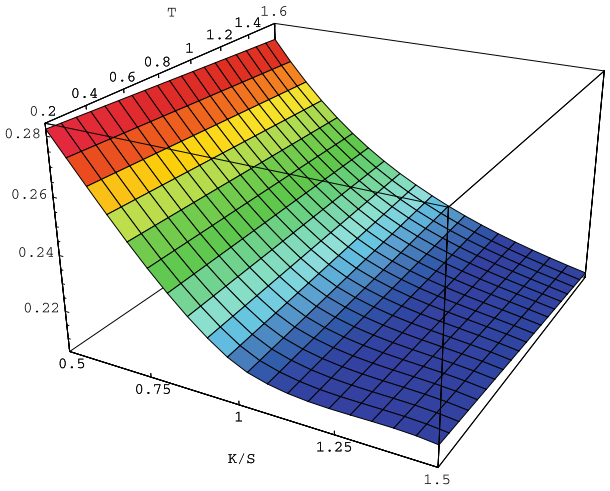

Fig. 12.1.5. Average S&P500 implied volatility surface

Consequently, the implied volatility term structure appears to be rather complex. Stylized facts on implied volatility surfaces are, for instance, documented in Dumas, Fleming & Whaley (1998), Schönbucher (1999), Ait-Sahalia & Lo (2000), Cont & da Fonseca (2002), Ledoit, Santa-Clara & Wolf (2003) and Le (2005). It would be highly desirable if an asset price model could also provide an economic interpretation for the volatility dynamics so that the trader can develop a reasoning behind this important market feature. In the following we shall discuss several volatility models which aim to match the type of implied volatility surface, as shown in Fig. 12.1.5.

12.2 Modified CEV Model

CEV Model

We present in this section a modification of the well-known *constant elasticity of variance* (CEV) *model*, as suggested in Heath & Platen (2002a). The CEV model assumes constant elasticity of variance for log-returns. This means that the volatility is a power function. This type of model seems to have first appeared in Cox (1975) and Cox & Ross (1976). It is a natural one-factor extension of the BS model that provides nonconstant stochastic volatilities and, thus, nonconstant implied volatilities. It has been adapted and applied more recently, for instance, in Andersen & Andreasen (2000), Lewis (2000), Lo, Yuen & Hui (2000) and Brigo & Mercurio (2005).

The classical risk neutral approach to the pricing of derivatives under the CEV model is described, for instance, in Beckers (1980) and Schroder (1989). It should be emphasized that these classical formulations typically assume a risk neutral dynamics of the underlying security, which in the case of the CEV

model may reach zero with strictly positive probability. This can lead to problems in the pricing of derivatives, see Lewis (2000) and Delbaen & Shirakawa (2002). The modified CEV model that we are going to consider does not have an equivalent risk neutral probability measure, as we shall see, and we apply real world pricing.

What makes the CEV type models attractive is that they easily generate a leverage effect, that is, a negative correlation between the index and its volatility, as discussed in Sect. 12.1.

Modified CEV Model

We consider a CFM, as introduced in Chap. 10, with one source of uncertainty $W = \{W_t,\, t \in [0, \infty)\}$, modeled by a standard Wiener process under the real world probability measure P on a filtered probability space $(\Omega, \mathcal{A}, \underline{\mathcal{A}}, P)$. The deterministic savings account S_t^0 at time t is given by the differential equation

$$dS_t^0 = r\, S_t^0\, dt \tag{12.2.1}$$

for $t \in [0, \infty)$ with $S_0^0 = 1$, where r denotes the constant short rate. By introducing the total market price of risk process $|\theta| = \{|\theta_t|,\, t \in [0, \infty)\}$, the GOP $S_t^{\delta_*}$ satisfies the SDE (12.1.1). Recall that the total market price of risk $|\theta_t|$ appears as the volatility at time t of the GOP. By introducing the drifted Wiener process $W_\theta = \{W_\theta(t),\, t \in [0, \infty)\}$ with

$$dW_\theta(t) = |\theta_t|\, dt + dW_t \tag{12.2.2}$$

we obtain from (12.1.1) for the GOP the SDE

$$dS_t^{\delta_*} = S_t^{\delta_*}\, (r\, dt + |\theta_t|\, dW_\theta(t)) \tag{12.2.3}$$

for $t \in [0, \infty)$.

To illustrate the kind of problem that may arise if there is no risk neutral probability measure under the classical formulation of the *modified CEV* model, we consider the case where the GOP volatility $|\theta_t|$ is specified in the form

$$|\theta_t| = (S_t^{\delta_*})^{a-1}\, \psi \tag{12.2.4}$$

for $t \in [0, \infty)$ with *exponent* $a \in (-\infty, \infty)$ and *scaling parameter* $\psi > 0$. In this case the appreciation rate of the GOP, see (12.1.1), is stochastic as long as $a \neq 1$.

We then have for the GOP by (12.2.3) and (12.2.4) the dynamics

$$dS_t^{\delta_*} = S_t^{\delta_*}\, r\, dt + (S_t^{\delta_*})^a\, \psi\, dW_\theta(t) \tag{12.2.5}$$

for $t \in [0, \infty)$. The existence and uniqueness of a solution of the SDE (12.2.5) is, in general, not automatically guaranteed without extra conditions on the

behavior of the process S^{δ_*} at zero, see Sect. 7.7 and Karatzas & Shreve (1991).

In (12.2.5), the process $W_\theta = \{W_\theta(t),\, t \in [0,\infty)\}$ is usually interpreted in the literature as a Wiener process under a risk neutral probability measure P_θ. Let us follow this interpretation for the moment. However, it will be shown that for $a < 1$ there is a major problem with the application of the risk neutral methodology. The scaling parameter ψ is, for simplicity, assumed to be constant.

Note that for the case $a = 1$ we have the BS model, which has a risk neutral probability measure P_ψ and constant market price of risk ψ. As we shall see shortly, this is the only case where considering a risk neutral version of the model makes sense.

By (12.1.1) and (12.2.4) the GOP satisfies the SDE

$$dS_t^{\delta_*} = \left(S_t^{\delta_*}\, r + (S_t^{\delta_*})^{2a-1}\, \psi^2\right) dt + (S_t^{\delta_*})^a\, \psi\, dW_t \tag{12.2.6}$$

for $t \in [0,\infty)$. The above choice (12.2.4) of the market price of risk contrasts with what is used in the classical formulation of the CEV model, see Cox & Ross (1976) and Schroder (1989). For this reason we refer to (12.2.6) as *modified CEV model*, which has been studied in Heath & Platen (2002a). As we shall see, the real world dynamics of the GOP, governed by (12.2.6), remains for $a < 1$ strictly positive. This is not the case for its hypothetical risk neutral dynamics when W_θ is interpreted as a Wiener process under P_θ, because S^{δ_*} may be absorbed at zero with strictly positive P_θ probability, as will become clear below.

Squared Bessel Process

We shall now show that the modified CEV model is closely related to squared Bessel processes, see Sect. 8.7. By application of the Itô formula we obtain from (12.2.6) for the quantity

$$X_t = \left(S_t^{\delta_*}\right)^{2\,(1-a)} \tag{12.2.7}$$

the SDE

$$dX_t = \left(2(1-a)\, r\, X_t + \psi^2\,(1-a)\,(3-2a)\right) dt + 2\,\psi\,(1-a)\,\sqrt{X_t}\, dW_t \tag{12.2.8}$$

for $t \in [0,\infty)$ with $X_0 = (S_0^{\delta_*})^{2\,(1-a)} > 0$. It follows from Sect. 8.7 that $X = \{X_t,\, t \in [0,\infty)\}$ is a time transformed, squared Bessel process of dimension

$$\delta = \frac{3-2\,a}{1-a} \tag{12.2.9}$$

for $a \neq 1$. Note that the SDE (12.2.8) has for $a \neq 1$ a nonnegative, unique strong solution, see Sect. 7.7, which for $a > 1$ we assume remains at zero when it reaches zero. By (12.2.7) the GOP can be expressed in the form

$$S_t^{\delta_*} = (X_t)^q, \tag{12.2.10}$$

where

$$q = \frac{1}{2\,(1-a)} \tag{12.2.11}$$

for $t \in [0, \infty)$ and $a \neq 1$. One notes that for extremely small $a < 1$ the dimension δ of the squared Bessel process X equals approximately two, which yields strongly leptokurtic log-returns for the GOP. However, for the exponent a when approaching one from below, the dimension δ tends to infinity, which yields lognormal dynamics for the GOP and, thus, Gaussian log-returns.

Hypothetical Risk Neutral Measure Transformation

In this setting the candidate Radon-Nikodym derivative process $\Lambda_\theta = \{\Lambda_\theta(t), t \in [0, \infty)\}$, which determines the *hypothetical risk neutral measure* P_θ for the pricing of options with maturity T with

$$\left.\frac{dP_\theta}{dP}\right|_{\mathcal{A}_T} = \Lambda_\theta(T), \tag{12.2.12}$$

is given by

$$\Lambda_\theta(t) = \frac{S_0^{\delta_*}}{S_t^{\delta_*}}\, S_t^0 \tag{12.2.13}$$

for $t \in [0, \infty)$, see (9.4.5). This means that by (12.2.10), the candidate Radon-Nikodym derivative equals the power of a time transformed, squared Bessel process of dimension δ, that is

$$\Lambda_\theta(t) = S_t^0 \left(\frac{X_0}{X_t}\right)^q \tag{12.2.14}$$

for $t \in [0, \infty)$, where q is given in (12.2.11).

Using (12.2.2) and (12.2.4) one can now rewrite the SDE (12.2.8) with respect to the drifted Wiener process W_θ, see (12.2.2), in the form

$$dX_t = \left(2\,(1-a)\,r\,X_t + \psi^2\,(1-a)(1-2\,a)\right)\,dt + 2\,\psi\,(1-a)\,\sqrt{X_t}\,dW_\theta(t) \tag{12.2.15}$$

for $t \in [0, \infty)$. Consequently, if one interprets the process X as a time transformed, squared Bessel process under a hypothetical risk neutral probability measure P_θ, then it would have the dimension

$$\delta_\theta = \frac{1-2\,a}{1-a} \tag{12.2.16}$$

for $a \neq 1$. In Fig. 12.2.1 we show the dimensions δ and δ_θ, see (12.2.9) and (12.2.16), of the above discussed time transformed, squared Bessel processes

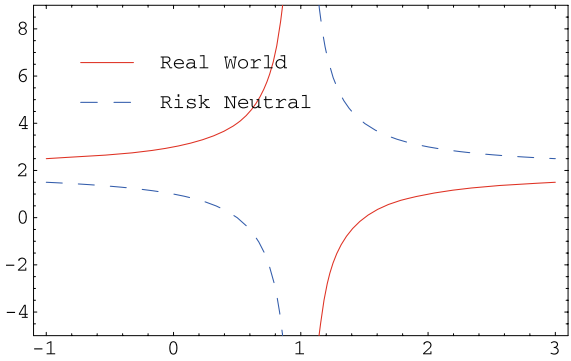

Fig. 12.2.1. Dimensions δ and δ_θ as a function of the exponent a

as a function of the exponent a, see Heath & Platen (2002b) and also Lewis (2000).

Note from Fig. 12.2.1 that if $a < 1$ then $\delta > 2$ and $\delta_\theta < 2$, and if $a > 1$ then $\delta < 2$ and $\delta_\theta > 2$. These inequalities follow from (12.2.9) and (12.2.16). It is known, see (8.7.7), that a time transformed, squared Bessel process with a dimension greater than two remains strictly positive. However, a time transformed, squared Bessel process with a dimension less than two hits zero with some strictly positive probability, see (8.7.8).

Hypothetical Risk Neutral Measure

In most of the previously mentioned literature one performs the modeling under a hypothetical risk neutral probability measure P_θ. This allows one to express the hypothetical risk neutral probability $P_\theta(A)$ for an event A in the form

$$P_\theta(A) = \int_A dP_\theta(\omega) = \int_A \frac{dP_\theta(\omega)}{dP(\omega)}\, dP(w) = \int_A \Lambda_\theta(T)\, dP(\omega), \qquad (12.2.17)$$

where $\Lambda_\theta(T)$ is the candidate Radon-Nikodym derivative described in (12.2.14) at time $T \in (0, \infty)$. Then one can ask for the total risk neutral measure. By (12.2.17) one obtains

$$P_\theta(\Omega) = \int_\Omega \Lambda_\theta(T)\, dP(\omega) = E\left(\Lambda_\theta(T) \,\middle|\, \mathcal{A}_0\right). \qquad (12.2.18)$$

If Λ_θ were an $(\underline{\mathcal{A}}, P)$-martingale, then $P_\theta(\Omega)$ would equal $\Lambda_\theta(0) = 1$ and P_θ would be a probability measure. However, for $a < 1$ it follows from (12.2.14) and Sect. 8.7 that Λ_θ is an $(\underline{\mathcal{A}}, P)$-strict local martingale, see (8.7.25), and, thus, by Lemma 5.2.3 an $(\underline{\mathcal{A}}, P)$-strict supermartingale. Consequently, we have for the total hypothetical risk neutral measure $P_\theta(\Omega) < 1$. This means that P_θ is for the given modified CEV model *not* a probability measure. Consequently,

for this model there does not exist an equivalent risk neutral probability measure P_θ for $a < 1$.

In addition, for $a > 1$ the dimension δ is less than two and the exponent q appearing in (12.2.10) is negative. It therefore follows from (8.7.8) that the GOP explodes for this parameter choice at some time with strictly positive P-probability. Consequently, the choice $a > 1$ does not lead to a viable model for the GOP. For this reason, we consider only the case $a < 1$ in the remainder of this section.

Real World Pricing

As we have seen previously, with its real world pricing concept the benchmark approach provides a consistent pricing framework without requiring the existence of an equivalent risk neutral probability measure. For $T \in [0, \infty)$ let $H = H(S_T^{\delta_*})$ denote a nonnegative payoff with

$$E\left(\frac{H(S_T^{\delta_*})}{S_T^{\delta_*}}\right) < \infty. \tag{12.2.19}$$

Recall from Sect. 9.1 that a price process is fair if, when expressed in units of the GOP, it is an $(\underline{\mathcal{A}}, P)$-martingale. Then the fair, benchmarked price $\hat{U}_H(t)$ at time t of this payoff is given by the conditional expectation

$$\hat{U}_H(t) = E\left(\frac{H(S_T^{\delta_*})}{S_T^{\delta_*}} \,\middle|\, \mathcal{A}_t\right) \tag{12.2.20}$$

for $t \in [0, T]$, see Definition 9.1.2. By using the transition density (8.7.9) of a squared Bessel process X of dimension $\delta = \frac{3-2a}{1-a}$ one can for some given payoff $H(S_T^{\delta_*})$ explicitly calculate the benchmarked price $\hat{U}_H(t)$ for any $t \in [0, T]$.

The fair price $U_H(t)$ of the payoff H, when expressed in units of the domestic currency, is then obtained by the real world pricing formula

$$U_H(t) = S_t^{\delta_*} \hat{U}_H(t) \tag{12.2.21}$$

for $t \in [0, T]$, see (9.1.31) or (10.4.1).

PDE for Benchmarked Pricing Function

As an alternative to the use of the transition density of the squared Bessel process X one can exploit the Markovianity of the GOP S^{δ_*}. This permits the application of the Feynman-Kac formula (9.7.3)–(9.7.4) to obtain the benchmarked price $\hat{U}_H(t) = \hat{u}_H(t, S_t^{\delta_*})$ as a function $\hat{u}_H : [0, T] \times [0, \infty) \to [0, \infty)$ of the time t and the value $S_t^{\delta_*}$ of the GOP. To formulate this method of calculation we define the operator L^0 on a sufficiently smooth function $f : [0, T) \times (0, \infty) \to \Re$ by

$$L^0 f(t,S) = \frac{\partial f(t,S)}{\partial t} + \left(r\,S + \psi^2\,S^{2a-1}\right)\frac{\partial f(t,S)}{\partial S} + \frac{1}{2}\,\psi^2\,S^{2a}\,\frac{\partial^2 f(t,S)}{\partial S^2} \tag{12.2.22}$$

for $(t,S) \in (0,T) \times (0,\infty)$.

Applying the above operator L^0 to the benchmarked pricing function $\hat{u}_H(\cdot,\cdot)$ by using (12.2.20), (12.2.6) and the Feynman-Kac formula, yields the PDE

$$L^0\,\hat{u}_H(t,S) = 0 \tag{12.2.23}$$

for $(t,S) \in (0,T) \times (0,\infty)$ with the terminal condition

$$\hat{u}_H(T,S) = \frac{H(S)}{S} \tag{12.2.24}$$

for $S \in (0,\infty)$. It remains to solve the PDE (12.2.23)–(12.2.24), which, for instance, can be achieved by a finite difference method, as will be described in Sect. 15.7.

Martingale Representation

From the Feynman-Kac formula it follows that the benchmarked pricing function $\hat{u}_H : [0,T] \times [0,\infty) \to [0,\infty)$ is differentiable with respect to time t and twice differentiable with respect to $S_t^{\delta_*}$ on $(0,T) \times (0,\infty)$. Consequently, by application of the Itô formula, using (12.2.6), we obtain the representation

$$\hat{u}_H(t, S_t^{\delta_*}) = \hat{u}_H(0, S_0^{\delta_*}) + \int_0^t (S_s^{\delta_*})^a\,\psi\,\frac{\partial \hat{u}_H(s, S_s^{\delta_*})}{\partial S^{\delta_*}}\,dW_s \tag{12.2.25}$$

for $t \in [0,T]$. This is the martingale representation of the benchmarked price, as discussed in Sect. 11.4. By Theorem 11.5.2 this representation provides the information about the hedge that enables one to replicate the payoff.

Hedge Portfolio

Obviously, by (12.2.1) and (12.2.6), the benchmarked savings account $\hat{S}_t^0$ satisfies by the Itô formula the SDE

$$d\hat{S}_t^0 = -S_t^0\,\left(S_t^{\delta_*}\right)^{a-2}\,\psi\,dW_t \tag{12.2.26}$$

for $t \in [0,\infty)$. Trivially, we have $d\hat{S}_t^{\delta_*} = 0$ for $t \in [0,\infty)$.

For a given payoff function $H(S_T^{\delta_*})$ we can construct a hedge portfolio consisting of $\delta_H^0(t)$ units of the savings account S_t^0 and $\delta_H^1(t)$ units of the GOP $S_t^{\delta_*}$. As one can see from (12.2.25) and (12.2.26), to construct a replicating portfolio we need to choose the hedge ratios according to the prescription

$$\delta_H^0(t) = -\frac{(S_t^{\delta_*})^2}{\hat{S}_t^0}\,\frac{\partial \hat{u}_H(t, S_t^{\delta_*})}{\partial S^{\delta_*}} \tag{12.2.27}$$

and

$$\delta_H^1(t) = \hat{u}_H(t, S_t^{\delta_*}) - \delta_H^0(t)\,\hat{S}_t^0 \tag{12.2.28}$$

for $t \in [0, T]$. This choice ensures that the value of the hedge portfolio, when measured in units of the domestic currency, equals the fair price $U_H(t) = u_H(t, S_t^{\delta_*})$ at time $t \in [0, T]$. That is

$$u_H(t, S_t^{\delta_*}) = \delta_H^0(t)\,S_t^0 + \delta_H^1(t)\,S_t^{\delta_*} \tag{12.2.29}$$

for $t \in [0, T]$. The benchmarked value of the hedge portfolio is, therefore, given by

$$\hat{u}_H(t, S_t^{\delta_*}) = \delta_H^0(t)\,\hat{S}_t^0 + \delta_H^1(t) \tag{12.2.30}$$

for $t \in [0, T]$. By (12.2.20) this hedge portfolio replicates the payoff at the maturity date T. Since it is a fair portfolio it provides by Corollary 10.4.2 the minimal hedge.

Benchmarked P&L

To illustrate the replication of the payoff, we define the *benchmarked* P&L $\hat{C}_H(t)$ for maintaining this hedge portfolio up to time $t \in [0, T]$. Similarly to (8.2.13) it equals the benchmarked value of the hedge portfolio minus the benchmarked gains from trade and the benchmarked initial value, that is,

$$\hat{C}_H(t) = \hat{u}_H(t, S_t^{\delta_*}) - \int_0^t \delta_H^0(s)\,d\hat{S}_s^0 - \hat{u}_H(0, S_0^{\delta_*}) \tag{12.2.31}$$

for $t \in [0, T]$. By combining (12.2.31), (12.2.27), (12.2.25) and (12.2.22) we see that

$$\hat{C}_H(t) = 0 \tag{12.2.32}$$

for all $t \in [0, T]$. This means that the benchmarked P&L for maintaining the hedge portfolio is always zero. Consequently, the P&L

$$C_H(t) = \hat{C}_H(t)\,S_t^{\delta_*} = 0 \tag{12.2.33}$$

equals zero for all times $t \in [0, T]$. Thus, the payoff $H(S_T^{\delta_*})$ can be perfectly hedged using the real world pricing formula (12.2.21) together with the hedging prescriptions (12.2.27) and (12.2.30).

Hedge Ratio

By using (12.2.27), (12.2.30) and (12.2.25) the hedge ratio $\delta_H^1(t)$ can be rewritten in the form

$$\delta_H^1(t) = \hat{u}_H(t, S_t^{\delta_*}) + S_t^{\delta_*}\,\frac{\partial \hat{u}_H(t, S_t^{\delta_*})}{\partial S^{\delta_*}} = \frac{\partial u_H(t, S_t^{\delta_*})}{\partial S^{\delta_*}} \tag{12.2.34}$$

for $t \in [0,T]$. Therefore, the number of units $\delta_H^1(t)$ held in the GOP at time $t \in [0,T]$ equals the delta hedge ratio obtained by calculating the partial derivative of the fair price with respect to the value of the underlying, that is the GOP. This is entirely analogous to what we obtained in Chap. 8 under the BS model. It is also analogous to what one obtains in a classical risk neutral hedging framework when using a savings account for hedging, see, for instance, Karatzas & Shreve (1998). Note, however, that the above benchmark methodology still works when no equivalent risk neutral probability measure exists, as is the case for the given modified CEV model.

Fair Zero Coupon Bond

The price $P_T(t, S_t^{\delta_*})$ at time $t \in [0,T]$ for the fair zero coupon bond that pays one unit of the domestic currency at maturity T is given as

$$P_T(t, S_t^{\delta_*}) = S_t^{\delta_*} \, \hat{P}_T(t, S_t^{\delta_*}) \tag{12.2.35}$$

for $t \in [0,T]$, see (9.1.34) and (10.4.1), with

$$\hat{P}_T(t, S_t^{\delta_*}) = E\left(\frac{1}{S_T^{\delta_*}} \,\Big|\, \mathcal{A}_t \right). \tag{12.2.36}$$

Note by (8.7.16) that the conditional expectation in (12.2.36) can be calculated explicitly. The following explicit bond pricing formula for the modified CEV model has been established in Miller & Platen (2008). By using the transition density (8.7.9) of a squared Bessel process of dimension $\delta > 2$ one obtains

$$P_T(t, S_t^{\delta_*}) = E\left(\frac{S_t^{\delta_*}}{S_T^{\delta_*}} \,\Big|\, \mathcal{A}_t \right) = \exp\{-r\,(T-t)\}\, \chi^2(\ell^*; \delta - 2) \tag{12.2.37}$$

for $t \in [0,T]$. Here $\chi^2(\cdot;\delta)$ is the central chi-square distribution function with δ degrees of freedom, see (1.2.11), where

$$\ell^* = \frac{2\,r\,(S_t^{\delta_*})^{2(1-a)}}{\psi^2\,(1-a)\,(1-\exp\{-2(1-a)\,r\,(T-t)\})}. \tag{12.2.38}$$

It is clear that

$$P_T(t, S_t^{\delta_*}) < \exp\{-r\,(T-t)\} \tag{12.2.39}$$

for all $t \in [0,T)$ and $S_t^{\delta_*} > 0$, because $\chi^2(\ell^*; \delta - 2)$ is the value of a chi-square distribution.

We remark that the function $\hat{P}_T(\cdot,\cdot)$ of the benchmarked fair zero coupon bond price satisfies the PDE

$$L^0\, \hat{P}_T(t,S) = 0 \tag{12.2.40}$$

for $(t, S) \in [0, T) \times (0, \infty)$ with terminal condition

$$\hat{P}_T(T, S) = \frac{1}{S} \tag{12.2.41}$$

for $S \in (0, \infty)$, see (12.2.23)–(12.2.24), where the operator L^0 is given in (12.2.22).

Savings Bond

The price process $u_H = \{u_H(t, S_t^{\delta_*}),\, t \in [0, \infty)\}$ in (12.2.28) is the only fair portfolio process, which perfectly replicates the payoff. However, as we shall see below, other nonnegative portfolio processes exist, which also perfectly replicate the payoff. As shown in Theorem 10.3.1, any benchmarked nonnegative portfolio process forms an $(\underline{\mathcal{A}}, P)$-supermartingale. From this it followed in Corollary 10.4.2 that the fair price, as obtained according to (12.2.29), yields the minimal price that permits perfect replication of the payoff. This will be verified for our case below.

Since we have assumed a constant short rate $r_t = r$ it is easy to introduce an artificial *savings bond* $P_T^* = \{P_T^*(t),\, t \in [0, \infty)\}$ with

$$P_T^*(t) = \frac{S_t^0}{S_T^0} = \exp\{-r\,(T - t)\} \tag{12.2.42}$$

for $t \in [0, T]$. By application of the Itô formula, it can be shown by (12.2.10), (12.2.8) and (12.2.42), that the benchmarked savings bond price process $\hat{P}_T^* = \{\hat{P}_T^*(t, S_t^{\delta_*}),\ t \in [0, T]\}$ with

$$\hat{P}_T^*(t, S_t^{\delta_*}) = \frac{P_T^*(t)}{S_t^{\delta_*}} = X_t^{-q}\, P_T^*(t) \tag{12.2.43}$$

satisfies the SDE

$$d\hat{P}_T^*(t, S_t^{\delta_*}) = -\hat{P}_T^*(t, S_t^{\delta_*})\, \frac{\psi}{\sqrt{X_t}}\, dW_t \tag{12.2.44}$$

for $t \in [0, T]$. Therefore, $\hat{P}_T^*$ forms an $(\underline{\mathcal{A}}, P)$-local martingale. Since a nonnegative, local martingale is an $(\underline{\mathcal{A}}, P)$-supermartingale, see Corollary (5.2.2), it follows that

$$\hat{P}_T^*(t, S_t^{\delta_*}) \geq E\left(\frac{1}{S_T^{\delta_*}} \,\middle|\, \mathcal{A}_t\right)$$

for $t \in [0, T]$. Therefore, by (12.2.35) and (12.2.43) we can deduce the inequality

$$P_T(t, S_t^{\delta_*}) = S_t^{\delta_*}\, E\left(\frac{1}{S_T^{\delta_*}} \,\middle|\, \mathcal{A}_t\right) \leq S_t^{\delta_*}\, \hat{P}_T^*(t, S_t^{\delta_*}) = P_T^*(t) \tag{12.2.45}$$

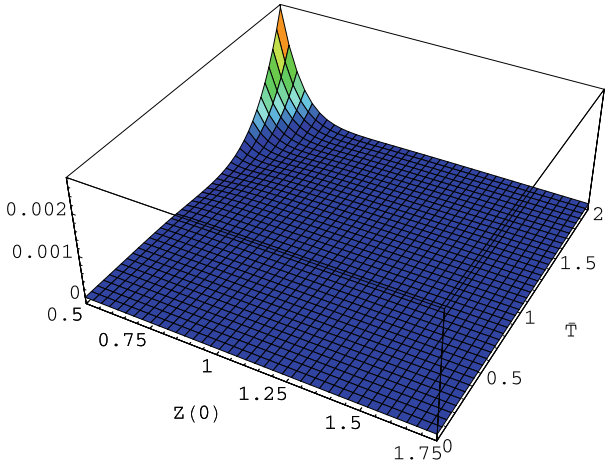

Fig. 12.2.2. Difference between savings and fair bond

for $t \in [0, T]$. This confirms our observation in (12.2.39) that the savings bond is at least as expensive as the fair zero coupon bond. In Fig. 12.2.2 we show the difference between the savings bond and the fair zero coupon bond for $a = -0.5$, $\psi = 0.2$ and $r = 0.04$. The savings bond is an unfair price process because when benchmarked it forms a strict supermartingale, see Exercise 12.6. However, it does not constitute an arbitrage in the sense of Definition 10.3.2.

Free Snack from Savings Bond

The above relation (12.2.45) poses an obvious question about the potential existence of arbitrage. As shown in (12.2.27)–(12.2.28), there exists a trading strategy which hedges the fair zero coupon bond under consideration. One may now form a trading strategy δ consisting of the aforementioned hedge, which is funded by borrowing the amount $P_T(0, S_0^{\delta_*})$ from a savings account at initiation. The portfolio value S_t^δ at time $t \in [0, T]$ is then given by the expression

$$S_t^\delta = P_T(t, S_t^{\delta_*}) - P_T(0, S_0^{\delta_*}) \exp\{-r\, t\}. \tag{12.2.46}$$

We observe that $S_0^\delta = 0$ and

$$S_T^\delta = 1 - P_T(0, S_0^{\delta_*}) \exp\{-r\, T\} > 0, \tag{12.2.47}$$

as well as

$$S_t^\delta \geq -P_T(0, S_0^{\delta_*}) \exp\{-r\, t\} \tag{12.2.48}$$

almost surely for all $t \in [0, T]$. Thus, δ is a strategy with a wealth process that is uniformly bounded from below. Since S_t^δ may become negative this portfolio is not covered by our arbitrage concept given in Definition 10.3.2. However, it is covered by the concept of free lunch with vanishing risk, see

Delbaen & Schachermayer (2006). Since we have in the given case a free lunch with vanishing risk it follows by the fundamental theorem of asset pricing of Delbaen & Schachermayer (1998) that the modified CEV model does not admit an equivalent risk neutral probability measure. This confirms what we observed already when we studied the strict supermartingale property of the candidate Radon-Nikodym derivative for the hypothetical risk neutral probability measure.

In Loewenstein & Willard (2000) a portfolio of the above kind is called a *free snack*. As we have seen, it rules out the existence of an equivalent risk neutral probability measure. However, it does not constitute an economic reason for dismissing the given model.

Benchmarked Savings Bond

Note that the pricing function of the *benchmarked savings bond* $\hat{P}_T^*(\cdot,\cdot)$ satisfies the PDE (12.2.23) with

$$L^0\,\hat{P}_T^*(t,S) = 0 \tag{12.2.49}$$

for $(t,S) \in [0,T) \times (0,\infty)$ and terminal condition

$$\hat{P}_T^*(T,S) = \frac{1}{S} \tag{12.2.50}$$

for $S \in (0,\infty)$. The PDE (12.2.40) with terminal condition (12.2.41) is the same as the one given in (12.2.49) and (12.2.50). Therefore, there is more than one solution to the PDE problem (12.2.49)–(12.2.50). This is related to the fact that the solution to this PDE is not fully determined without specification of its behavior along the spatial boundary at zero. From the absence of arbitrage in the sense of Definition 10.3.2 it follows from (10.3.4) that any nonnegative portfolio that reaches zero remains at zero after that time. For this reason the spatial boundary condition where S reaches zero must be that of absorption.

The above savings bond provides a perfect hedge via a self-financing portfolio that replicates one monetary unit at maturity T. Note however that this is not the minimal possible hedge portfolio. The fair zero coupon bond portfolio, given by the price (12.2.35), provides the minimal hedge since its benchmarked value forms a martingale while the benchmarked savings bond is a strict supermartingale.

European Call Option

For a *European call option* on the GOP with strike K and maturity T the benchmarked fair price $\hat{c}_{T,K}(t, S_t^{\delta_*})$ at time t is given by the formula

$$\hat{c}_{T,K}(t, S_t^{\delta_*}) = E\left(\frac{(S_T^{\delta_*} - K)^+}{S_T^{\delta_*}} \,\middle|\, \mathcal{A}_t\right) = E\left(\left(1 - \frac{K}{S_T^{\delta_*}}\right)^+ \,\middle|\, \mathcal{A}_t\right) \tag{12.2.51}$$

for $t \in [0, T]$. Note that the conditional expectation used in (12.2.51) is finite because the payoff $(1 - \frac{K}{S_T^{\delta_*}})^+$ is bounded. Thus, the inequality (12.2.19) for the European call payoff is satisfied. The corresponding fair price $c_{T,K}(t, S_t^{\delta_*})$, see (12.2.21), takes the form by the real world pricing formula (9.1.34) and (10.4.1)

$$c_{T,K}(t, S_t^{\delta_*}) = S_t^{\delta_*} \, \hat{c}_{T,K}(t, S_t^{\delta_*}) \tag{12.2.52}$$

for $t \in [0, T]$.

By (12.2.23) the function $\hat{c}_{T,K}(\cdot, \cdot)$ satisfies the PDE (12.2.23) with terminal condition

$$\hat{c}_{T,K}(T, S) = \hat{H}(S) = \left(1 - \frac{K}{S}\right)^+ \tag{12.2.53}$$

for $S \in (0, \infty)$, which can be solved numerically.

Alternatively, one can calculate the benchmarked European call price by exploiting the known transition density of the squared Bessel process X. This yields by (8.7.9), see Miller & Platen (2008), the explicit expression

$$\hat{c}_{T,K}(t, S_t^{\delta_*}) = (1 - \chi^2(u^*; \delta, \ell^*)) - \frac{K}{S_t^{\delta_*}} \, \exp\{-r\,(T-t)\}\, \chi^2(\ell^*; \delta - 2, u^*), \tag{12.2.54}$$

where

$$u^* = \frac{2\, r\, K^{2(1-a)}}{\psi^2\,(1-a)\,(\exp\{2(1-a)\, r\,(T-t)\} - 1)} \tag{12.2.55}$$

and ℓ^* is as in (12.2.38) for $t \in (0, T]$ and $\chi^2(\cdot; \delta, \cdot)$ is the non-central chi-square distribution (1.2.13) with degrees of freedom δ. Now, when using the previous notation we obtain the explicit European call pricing formula

$$c_{T,K}(t, S_t^{\delta_*}) = S_t^{\delta_*} \left(1 - \chi^2(u^*; \delta, \ell^*)\right) - K \, \exp\{-r\,(T-t)\}\, \chi^2(\ell^*; \delta - 2, u^*) \tag{12.2.56}$$

for the modified CEV model, see Miller & Platen (2008). This explicit pricing formula is equivalent to similar CEV call option pricing formulas that one can find in Cox & Ross (1976), Beckers (1980), Schroder (1989), Cox (1996), Shaw (1998) and Delbaen & Shirakawa (2002). The important difference, however, is that an equivalent risk neutral probability measure does not exist for the modified CEV model. We shall discuss this issue further below.

According to (12.1.5) one can visualize a European call price efficiently by its implied volatility. For an exponent $a = -0.5$, that is with dimension $\delta \approx 2.67$, $\psi = 0.2$, a constant interest rate $r = 0.04$ and maturity dates of up to two years, Fig. 12.2.3 displays the corresponding implied volatility surface that results from the fair call option price using different values of the strike K and time t for fixed value of $S_t^{\delta_*} = 1$. In Fig. 12.2.3 we see negatively skewed implied volatilities. Note that we use here the fair zero coupon bond as discount factor for the inversion of the Black-Scholes formula when calculating implied volatilities. More precisely, we use the substitute short rate for a European call option with maturity T

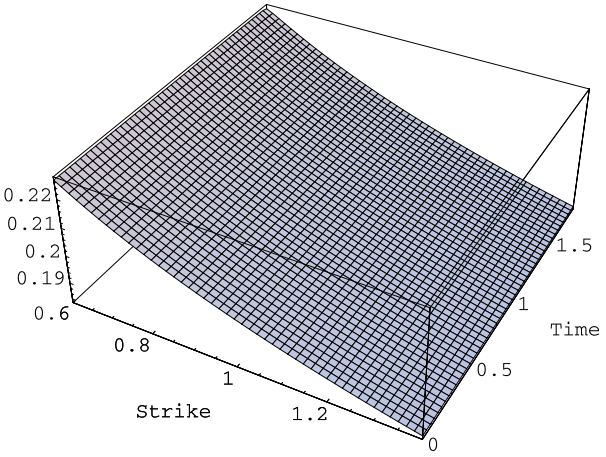

Fig. 12.2.3. Implied volatilities for fair European call prices

$$\hat{r} = -\frac{1}{T-t}\,\ln(P_T(t, S_t^{\delta_*})) = \frac{1}{T-t}\int_t^T f(t,s)ds \tag{12.2.57}$$

when calculating implied volatilities. Here $f(t,s)$ denotes the forward rate at time t for the maturity s, see (10.4.12). We emphasize that it is important to make the above adjustment. Otherwise, implied put and call volatilities do not match.

European Put Option

Similarly, one can also compute the fair European put option price

$$p_{T,K}(t, S_t^{\delta_*}) = S_t^{\delta_*}\, E\left(\left(\frac{K}{S_T^{\delta_*}} - 1\right)^+ \Big| \mathcal{A}_t\right) \tag{12.2.58}$$

for $t \in [0,T]$, which has by application of the transition density (8.7.9) the explicit form

$$\begin{aligned} p_{T,K}(t, S_t^{\delta_*}) = &-S_t^{\delta_*}\,\chi^2(u^*;\delta,\ell^*) + K\,\exp\{-r\,(T-t)\} \\ &\times \left(\chi^2(\ell^*;\delta-2) - \chi^2(\ell^*;\delta-2,u^*)\right) \end{aligned} \tag{12.2.59}$$

for $t \in [0,T]$ with the notation (12.2.55)–(12.2.38). This explicit, fair European put pricing formula for the modified CEV model, see Miller & Platen (2008), is clearly different from the type of put pricing formulas that one would obtain from Cox & Ross (1976), Beckers (1980), Schroder (1989), Cox (1996) or Shaw (1998). The reason is that these authors priced a CEV model under the assumption that it has an equivalent risk neutral probability measure. Their benchmarked put prices are strict supermartingales. The modified

CEV model does not have an equivalent risk neutral probability measure and its benchmarked fair put prices are martingales.

In Lewis (2000) some rules are proposed that aim to account for the differences that arise when constructing some hypothetical risk neutral prices in models like the CEV model. Unfortunately, this approach appears to lead to conceptual problems when going beyond standard put and call options. The real world pricing concept of the benchmark approach also applies to the pricing under any reasonable model that has a GOP.

Fair Put-Call Parity

By using the corresponding fair zero coupon bond price with maturity T the *fair put-call parity* is satisfied, that is, the following relation holds

$$p_{T,K}(t, S_t^{\delta_*}) = c_{T,K}(t, S_t^{\delta_*}) - S_t^{\delta_*} + K\, P_T(t, S_t^{\delta_*}) \tag{12.2.60}$$

for $t \in [0, T]$. However, by (12.2.39) we have

$$p_{T,K}(t, S_t^{\delta_*}) < c_{T,K}(t, S_t^{\delta_*}) - S_t^{\delta_*} + K\, \exp\{-r\,(T-t)\} \tag{12.2.61}$$

for $t \in [0, T)$ and $S_t^{\delta_*} > 0$. This means, when using the savings bond instead of the fair bond in (12.2.60), put-call parity does not hold. Note that this effect arises here even in a model with constant interest rates.

As already indicated, since we use the fair zero coupon bond price as the discount factor for the computation of implied volatilities from the Black-Scholes formula, the implied volatilities of fair puts equal those of corresponding fair calls. However, if one would use the savings bond in such calculations as discount factor, then differences between the implied volatilities for puts and calls would emerge.

Comparison to Hypothetical Risk Neutral Prices

Let us now compare the above results with those that one would obtain under formal application of the standard risk neutral pricing methodology. This means we are for a moment neglecting the fact that there does not exist an equivalent risk neutral probability measure for the given modified CEV model.

We define the hypothetical risk neutral price $c^*_{T,K}(t, S_t^{\delta_*})$ at time t of a European call option on the GOP with strike K and maturity T by $c^*_{T,K}(t, S_t^{\delta_*})$ for $t \in [0, T]$. The benchmarked hypothetical risk neutral call price

$$\hat{c}^*_{T,K}(t, S_t^{\delta_*}) = \frac{c^*_{T,K}(t, S_t^{\delta_*})}{S_t^{\delta_*}} \tag{12.2.62}$$

forms an $(\underline{\mathcal{A}}, P)$-local martingale, as all benchmarked portfolio processes in a CFM. One notes the important fact that its benchmarked payoff is bounded.

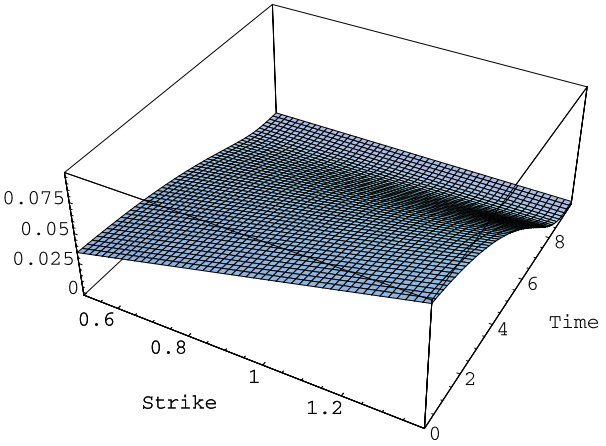

Fig. 12.2.4. Difference between hypothetical risk neutral and fair put prices

Therefore, the benchmarked hypothetical risk neutral price $\hat{c}^*_{T,K}(\cdot,\cdot)$ is uniformly bounded. By Lemma 5.2.2 (ii) it follows that bounded local martingales are martingales. Therefore, $\hat{c}^*_{T,K}$ forms a martingale such that

$$\hat{c}^*_{T,K}(t, S^{\delta_*}_t) = \hat{c}_{T,K}(t, S^{\delta_*}_t)$$

and thus

$$c^*_{T,K}(t, S^{\delta_*}_t) = c_{T,K}(t, S^{\delta_*}_t) \tag{12.2.63}$$

for all $t \in [0, T]$. This means that hypothetical risk neutral and fair call option prices coincide in the given case.

We now introduce the hypothetical risk neutral put price by the corresponding hypothetical risk neutral put-call parity relation

$$p^*_{T,K}(t, S^{\delta_*}_t) = c^*_{T,K}(t, S^{\delta_*}_t) - S^{\delta_*}_t + K\, P^*_T(t) \tag{12.2.64}$$

for $t \in [0, T]$, where $P^*_T(\cdot)$ is the savings bond, see (12.2.42). By applying (12.2.61) and (12.2.64) it can be inferred that

$$p_{T,K}(t, S^{\delta_*}_t) < p^*_{T,K}(t, S^{\delta_*}_t) \tag{12.2.65}$$

for all $t \in [0, T)$. This means that the fair put price is less than or equal to the hypothetical risk neutral put price.

Figure 12.2.4 shows the difference between the hypothetical risk neutral and the fair European put price as a function of the strike K and time t for the same parameter values used in Fig. 12.2.3. Note that these differences are always nonnegative, see (12.2.65). This visualizes again the fact that fair prices are the minimal prices that replicate a contingent claim, see Corollary 10.4.2.

Difference in Asymptotic Put Prices

When considering the above analysis it becomes clear that differences between fair and hypothetical risk neutral prices arise when the payoff is not vanishing for vanishing GOP. In such a case the risk neutral pricing methodology suggests some prices that contradict economic reasoning. There always exists a corresponding fair price that allows a perfect hedge which is less or equal to the hypothetical risk neutral price.

Now, we shall demonstrate that the differences between fair prices and hypothetical risk neutral prices can become extreme if the underlying GOP value tends towards zero. One can show by the conditional moment estimate (8.7.16) for the benchmarked, fair zero coupon bond, see (12.2.36) and (12.2.10), when the GOP comes close to zero, that

$$\lim_{S_t^{\delta_*}\to 0} \hat{P}_T(t, S_t^{\delta_*}) \stackrel{\text{a.s.}}{=} \lim_{X_t\to 0} E\left((X_T)^{-q} \,\middle|\, \mathcal{A}_t\right) < \infty \tag{12.2.66}$$

so that

$$\lim_{S_t^{\delta_*}\to 0} P_T(t, S_t^{\delta_*}) \stackrel{\text{a.s.}}{=} \lim_{S_t^{\delta_*}\to 0} S_t^{\delta_*}\, \hat{P}_T(t, S_t^{\delta_*}) = 0 \tag{12.2.67}$$

for $t \in [0, T]$ and $T \in (0, \infty)$. In addition, since

$$\lim_{S_t^{\delta_*}\to 0} c_{T,K}(t, S_t^{\delta_*}) \stackrel{\text{a.s.}}{=} \lim_{S_t^{\delta_*}\to 0} S_t^{\delta_*}\, \hat{c}_{T,K}(t, S_t^{\delta_*}) = 0, \tag{12.2.68}$$

by application of the fair put-call parity relation (12.2.60) we see for the fair put price that

$$\lim_{S_t^{\delta_*}\to 0} p_{T,K}(t, S_t^{\delta_*}) \stackrel{\text{a.s.}}{=} 0 \tag{12.2.69}$$

for $t \in [0, T]$. However, from the hypothetical risk neutral put-call parity relation (12.2.64) together with (12.2.63), (12.2.68) and (12.2.42) it can be seen that the corresponding hypothetical risk neutral put price satisfies for vanishing GOP the limit condition

$$\lim_{S_t^{\delta_*}\to 0} p^*_{T,K}(t, S_t^{\delta_*}) \stackrel{\text{a.s.}}{=} K\, \frac{S_t^0}{S_T^0} > 0 \tag{12.2.70}$$

for $t \in [0, T]$. By comparing (12.2.69) and (12.2.70), we note a difference between the behavior of the fair and hypothetical risk neutral put prices as the GOP comes close to zero. We emphasize again that the fair put price is, in economic terms, the correct price for this contingent claim as it can be perfectly hedged using the hedge ratios (12.2.27) and (12.2.30) and there is no lower put price which could be used for replication. We emphasize that in both cases the put payoff is replicated by a self-financing hedge portfolio.

The above study of the modified CEV model signals that one has to be very careful in the pricing and hedging under stochastic volatility. This is of particular relevance if an index model attempts to capture the leverage effect

where volatility increases when the index value decreases. One can expect that this results in effects similar to those described above. For a realistic model the volatility has to become large when the index attains small values to be able to reflect the economically relevant risk involved. This suggests that realistic index models can be expected to face the above experienced problems when applying the risk neutral methodology.

12.3 Local Volatility Models

LV Models

As we have seen in Sect. 12.1, the existence of implied volatility skews for options on indices is well documented. A natural one-factor extension of the BS model is obtained by introducing *local volatility* (LV) *models*. This means that the volatility is allowed to change as a function of the underlying and time. The resulting LV models have attracted the interest of many researchers and practitioners. They were pioneered by Dupire (1992, 1993, 1994) and Derman & Kani (1994a, 1994b) and have been widely used in practice. However, in this literature one typically assumes the existence of a risk neutral probability measure. This could be problematic since the modified CEV model, considered in the previous section, is a special case of an LV model. Another LV model is the MMM proposed in Platen (2001), which was mentioned in Sect. 7.5. We shall see in the next chapter that it does not have an equivalent risk neutral probability measure. Therefore, in this section we apply again real world pricing to obtain derivative prices.

In the first part of this section it will be our aim to estimate the real world transition density of the underlying index from observed call option prices and also its local volatility function. Typically, in the literature on LV models one extracts risk neutral transition densities from observed option prices, see Dupire (1994). This does not make sense for models that do not have an equivalent risk neutral probability measure. Therefore, it will be our aim to estimate the real world transition density without relying on the existence of an equivalent risk neutral probability measure.

Local Volatility

Let us consider a CFM with GOP process $S^{\delta_*} = \{S_t^{\delta_*}, t \in [0, \infty)\}$, which we interpret, similarly to the previous section, as a diversified accumulation index. For simplicity, the short rate $r_t = r$ is assumed to be constant. We say that the GOP $S_t^{\delta_*}$ follows an LV model if it satisfies an SDE of the form

$$dS_t^{\delta_*} = S_t^{\delta_*} \left(\left(r + \sigma^2(t, S_t^{\delta_*}) \right) dt + \sigma(t, S_t^{\delta_*})\, dW_t \right) \tag{12.3.1}$$

for $t \in [0, \infty)$, see (10.2.8). This formulation of the GOP dynamics incorporates the total market price of risk $|\theta_t|$, as a function of time t and underlying security $S_t^{\delta_*}$, in the form of the *local volatility* (LV)

$$|\theta_t| = \sigma(t, S_t^{\delta_*}) \tag{12.3.2}$$

for $t \in [0, \infty)$. The specific structural assumption here is that the total market price of risk depends on the underlying security and time. The choice of the LV function characterizes the selected LV model. Here $W = \{W_t, t \in [0, \infty)\}$ denotes a standard Wiener process on a filtered probability space $(\Omega, \mathcal{A}, \underline{\mathcal{A}}, P)$, where P is the real world probability measure. Furthermore, we assume that a unique strong solution of the SDE (12.3.1) exists, see Sect. 7.7, which is not trivial for certain classes of LV functions. In cases, where $S_t^{\delta_*}$ may reach zero, we choose zero as an absorbing boundary, similarly as in (7.7.18).

LV Function

Under an LV model it is assumed that the volatility $\sigma(t, S_t^{\delta_*})$ is generated by a given *LV function* $\sigma : [0, \infty) \times [0, \infty) \to [0, \infty]$, which is a deterministic function of time and the underlying security.

If the *volatility process* $\sigma = \{\sigma(t, S_t^{\delta_*}), t \in [0, \infty)\}$ is deterministic, then we have a BS model for S^{δ_*}. The modified CEV model, considered in the previous section, has as LV function the power function

$$\sigma(t, S_t^{\delta_*}) = (S_t^{\delta_*})^{a-1} \psi \tag{12.3.3}$$

for some exponent $a \in (-\infty, 1)$ and constant scaling parameter ψ.

Another LV model is obtained by the stylized version of the MMM, mentioned in Sect. 7.5. Here the LV function has the form

$$\sigma(t, S_t^{\delta_*}) = \sqrt{\frac{\alpha_0 \, \exp\{(r+\eta)\, t\}}{S_t^{\delta_*}}}, \tag{12.3.4}$$

with constant net growth rate $\eta > 0$ and initial parameter $\alpha_0 > 0$. In this case the GOP can be modeled as

$$S_t^{\delta_*} = Y_t \, \alpha_0 \, \exp\{(r+\eta)\, t\} \tag{12.3.5}$$

for $t \in [0, \infty)$ with parameters $\alpha_0, \eta, r > 0$. In (12.3.5) $Y = \{Y_t, t \in [0, \infty)\}$ is a square root process of dimension four, which satisfies the SDE

$$dY_t = (1 - \eta \, Y_t)\, dt + \sqrt{Y_t}\, dW_t \tag{12.3.6}$$

for $t \in [0, \infty)$, see (7.5.16), with $Y_0 = \frac{S_0^{\delta_*}}{\alpha_0} > 0$. One notes that the LV function (12.3.4) of the stylized MMM can be expressed simply as a function of the value of the square root process Y. That is, by (12.3.4) and (12.3.5) we can write

$$\sigma(t, S_t^{\delta_*}) = \frac{1}{\sqrt{Y_t}} \tag{12.3.7}$$

for $t \in [0, \infty)$. Consequently, the squared volatility is the inverse of a square root (SR) process. Such an SR process is known to have as stationary density a gamma density, see Sect. 4.5. Therefore, in the case of the stylized MMM the volatility has a stationary density and, thus, allows us to model some kind of an equilibrium.

Benchmarked Savings Account

The benchmarked savings account process $\hat{S}^0 = \{\hat{S}_t^0,\, t \in [0, \infty)\}$ is again given by the ratio

$$\hat{S}_t^0 = \frac{S_t^0}{S_t^{\delta_*}}. \tag{12.3.8}$$

For the LV model it satisfies, by an application of the Itô formula together with (12.3.1), the driftless SDE

$$d\hat{S}_t^0 = -\hat{S}_t^0\, \sigma\left(t, \frac{S_t^0}{\hat{S}_t^0}\right) dW_t \tag{12.3.9}$$

for $t \in [0, \infty)$. Since a nonnegative, local martingale is a supermartingale, see Lemma 5.2.2 (i) and Theorem 10.3.1, the benchmarked savings account $\hat{S}^0$ is a supermartingale. Recall from Sect. 9.4 that the candidate Radon-Nikodym derivative process $\Lambda = \{\Lambda_t,\, t \in [0, \infty)\}$ of the hypothetical risk neutral probability measure is given by the normalized benchmarked savings account $\Lambda = \{\Lambda_t,\, t \in [0, \infty)\}$ with

$$\Lambda_t = \frac{\hat{S}_t^0}{\hat{S}_0^0} = \exp\left\{-\frac{1}{2}\int_0^t \sigma(s, S_s^{\delta_*})^2\, ds - \int_0^t \sigma(s, S_s^{\delta_*})\, dW_s\right\} \tag{12.3.10}$$

for $t \in [0, \infty)$. We have already seen for the modified CEV model that Λ can become a strict $(\underline{\mathcal{A}}, P)$-supermartingale. Therefore, an equivalent risk neutral probability measure may not exist for a range of LV models.

Real World Pricing under an LV Model

Let $H = H(S_T^{\delta_*})$ denote a nonnegative payoff with maturity date $T \in (0, \infty)$. Then its benchmarked fair price $\hat{U}_H(t)$ at time $t \in [0, T]$ is given by the conditional expectation

$$\hat{U}_H(t) = E\left(\frac{H(S_T^{\delta_*})}{S_T^{\delta_*}} \,\middle|\, \mathcal{A}_t\right) \tag{12.3.11}$$

for $t \in [0, T]$, see Definition 9.1.2. The corresponding fair price $U_H(t)$ at time t, expressed in units of the domestic currency, is then

$$U_H(t) = S_t^{\delta_*} \hat{U}_H(t) \tag{12.3.12}$$

for $t \in [0, T]$, which is the real world pricing formula. Note that under an LV model S^{δ_*} is a diffusion process and, thus, Markovian. For a sufficiently smooth function $f : [0, T] \times (0, \infty) \to \Re$ define the operator L^0 by the expression

$$L^0 f(t, S) = \frac{\partial f(t, S)}{\partial t} + (r + \sigma^2(t, S)) S \frac{\partial f(t, S)}{\partial S} + \frac{1}{2} \sigma^2(t, S) S^2 \frac{\partial^2 f(t, S)}{\partial S^2} \tag{12.3.13}$$

for $(t, S) \in (0, T) \times (0, \infty)$. Using (12.3.11) and (12.3.1) it follows by the Feynman-Kac formula (9.7.3)–(9.7.5) that the benchmarked fair pricing function $\hat{u}_H(\cdot, \cdot)$ with $\hat{u}_H(t, S_t^{\delta_*}) = \hat{U}_H(t)$ satisfies the PDE

$$L^0 \hat{u}_H(t, S) = 0 \tag{12.3.14}$$

for $(t, S) \in (0, T) \times (0, \infty)$ with terminal condition

$$\hat{u}_H(T, S) = \frac{H(S)}{S} \tag{12.3.15}$$

for $S \in (0, \infty)$.

The benchmarked fair pricing function $\hat{u}_H(\cdot, \cdot)$ is uniquely determined by (12.3.11) and satisfies the PDE (12.3.14) with terminal condition (12.3.15) as its minimal solution. As we have noticed from the modified CEV model, one needs to be aware of the fact that for certain types of payoffs the solution to this PDE may not be unique. This was, for instance, the case for zero coupon bonds and European puts. These are payoffs with nonvanishing value when the GOP reaches zero. However, we emphasize that there is only one minimal solution to the PDE (12.3.14)–(12.3.15), which is given by the benchmarked fair pricing function. In this case the boundary for $S \to 0$ is absorbing. This ensures the absence of arbitrage in the sense of Definition 10.3.2, because benchmarked nonnegative portfolios that reach zero stay at zero in a CFM.

For the fair price of $H(S_T^{\delta_*})$ a corresponding self-financing hedge portfolio, which replicates the payoff, can be constructed, similarly as in the previous section. If the benchmarked fair pricing function $\hat{u}_H(\cdot, \cdot)$ is sufficiently smooth, then we have by application of the Itô formula a martingale representation of the form

$$\frac{H(S_T^{\delta_*})}{S_T^{\delta_*}} = \hat{u}_H(t, S_t^{\delta_*}) + \int_t^T \frac{\partial \hat{u}_H(s, S_s^{\delta_*})}{\partial S^{\delta_*}} S_s^{\delta_*} \sigma(s, S_s^{\delta_*}) \, dW_s \tag{12.3.16}$$

for $t \in [0, T)$, see (11.5.3) and (12.2.25). One can form a hedge portfolio, see Theorem 11.5.2, consisting of $\delta_H^0(t)$ units of the domestic savings account and $\delta_H^1(t)$ units of the GOP at time t. By comparing (12.3.16) with the SDE for a benchmarked portfolio $\hat{S}^\delta$ one obtains the hedge ratios

$$\delta_H^0(t) = -\frac{(S_t^{\delta_*})^2}{S_t^0} \frac{\partial \hat{u}_H(t, S_t^{\delta_*})}{\partial S^{\delta_*}} \tag{12.3.17}$$

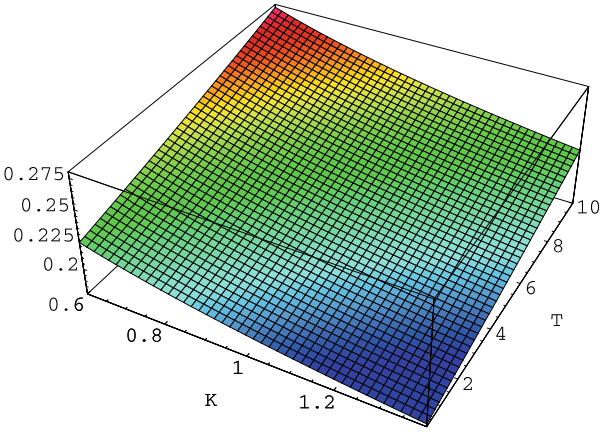

Fig. 12.3.1. Implied volatility surface for the stylized MMM

and

$$\delta_H^1(t) = \hat{u}_H(t, S_t^{\delta_*}) - \delta_H^0(t)\,\frac{S_t^0}{S_t^{\delta_*}} \tag{12.3.18}$$

for $t \in [0, T)$. These generalize the equations (12.2.27) and (12.2.28). This hedge portfolio replicates the payoff $H(S_T^{\delta_*})$. It provides perfect replication in the sense that the corresponding P&L remains zero, see (12.2.33). The portfolio value forms the minimal possible value since its benchmarked value is a martingale and coincides with the payoff at maturity T.

European Calls

If we denote by K the strike price of a European call option with maturity T, then at time t the corresponding *fair call option price* $c(t, S_t^{\delta_*}, T, K)$ satisfies the relation

$$c(t, S_t^{\delta_*}, T, K) = S_t^{\delta_*}\, E\left(\left(1 - \frac{K}{S_T^{\delta_*}}\right)^+ \,\middle|\, \mathcal{A}_t\right) \tag{12.3.19}$$

for $t \in [0, T]$.

Instead of the European call option prices their corresponding implied volatilities give a better view of the option market. We have shown in Fig. 12.2.3 the implied volatility surface for European calls, which results from the modified CEV model as a function of the strike and time to maturity. To provide another example we show in Fig. 12.3.1 the implied volatility surface's dependence on T and K for a fair call option under the stylized MMM given in Sect. 7.5, with $r = 0.04$, $\eta = 0.048$, $\alpha_0 = 0.03827$, and $S_0^{\delta_*} = 1$. In Fig. 12.3.1 we observe a pronounced negative skew. The term structure of implied volatility is characterized here by a gradual increase in at-the-money implied volatilities over time. Note that we take here, as in the previous section, the fair

zero coupon bond as discount factor when calculating implied volatilities, see (12.2.57). This means that we adjust in the Black-Scholes formula the short rate to

$$\hat{r} = \frac{-1}{T-t} \ln(P(t,T)) \tag{12.3.20}$$

for calculating implied volatilities.

Implied Transition Density of the GOP

We shall now demonstrate that it is, in principle, possible to estimate from observed option prices the transition probability density of the underlying GOP under an LV model. Let us denote by $p_{\hat{S}^0}(t, \hat{S}^0_t; T, \hat{S}^0_T)$ the transition density of the benchmarked savings account process $\hat{S}^0$ under the real world probability measure P. For convenient presentation we define the quantity

$$u(t, \hat{S}^0_t, T, \kappa) = \kappa \, \hat{c}_{T,K}(t, S^{\delta_*}_t) = \frac{S^0_T}{K \, S^{\delta_*}_t} \, c(t, S^{\delta_*}_t, T, K) \tag{12.3.21}$$

with the deterministic value

$$\kappa = \frac{S^0_T}{K}. \tag{12.3.22}$$

By (12.3.19) together with (12.3.8) this equation can be rewritten in the form

$$u(t, \hat{S}^0_t, T, \kappa) = E\left(\left(\kappa - \hat{S}^0_T \right)^+ \Big| \mathcal{A}_t \right). \tag{12.3.23}$$

Using an idea of Breeden & Litzenberger (1978), which was also applied by Dupire (1993) and Derman & Kani (1994b) in the risk neutral setting, it follows from (12.3.23) that

$$\begin{aligned} \frac{\partial}{\partial \kappa} u(t, \hat{S}^0_t, T, \kappa) &= \frac{\partial}{\partial \kappa} \int_0^\kappa (\kappa - y) \, p_{\hat{S}^0}(t, \hat{S}^0_t; T, y) \, dy \\ &= \int_0^\kappa p_{\hat{S}^0}(t, \hat{S}^0_t; T, y) \, dy. \end{aligned} \tag{12.3.24}$$

This allows us to express the real world transition density $p_{\hat{S}^0}$ in the form

$$p_{\hat{S}^0}(t, \hat{S}^0_t; T, \kappa) = \frac{\partial^2}{\partial \kappa^2} u(t, \hat{S}^0_t, T, \kappa) \tag{12.3.25}$$

for $t \in [0, T]$. By using (12.3.22) and (12.3.21) and calculating the partial derivative of u in terms of partial derivatives of the call pricing function c given in (12.3.19), the transition density $p_{\hat{S}^0}$ in (12.3.25) can be equivalently expressed in the form

$$p_{\hat{S}^0}(t, \hat{S}^0_t; T, \kappa) = \frac{K^3}{S^0_T \, S^{\delta_*}_t} \, \frac{\partial^2}{\partial K^2} \, c(t, S^{\delta_*}_t, T, K) \tag{12.3.26}$$

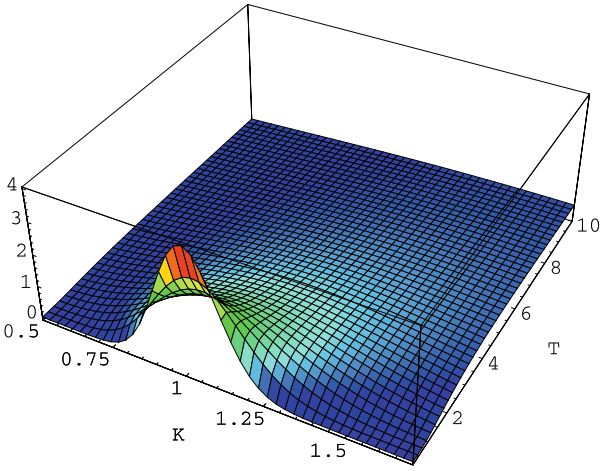

Fig. 12.3.2. Implied transition density obtained from CEV call option prices

for $t \in [0, T]$.

Let $p_{S^{\delta_*}}(t, S_t^{\delta_*}; T, K)$ denote the transition density for the GOP process S^{δ_*} under the real world probability measure P. Then the following result can be directly obtained by using the transformation (12.3.8) and formulas (12.3.25) and (12.3.26).

Lemma 12.3.1. *The transition density $p_{S^{\delta_*}}$ is of the form*

$$p_{S^{\delta_*}}(t, S_t^{\delta_*}; T, K) = \frac{K}{S_t^{\delta_*}} \frac{\partial^2}{\partial K^2} c(t, S_t^{\delta_*}, T, K) \tag{12.3.27}$$

for $t \in [0, T]$.

Consequently, by assuming the availability of a continuum of European call option prices with respect to strike and time to maturity we can theoretically infer the real world transition density of the GOP. This is different to most results in the literature where one infers risk neutral transition densities. As we have seen earlier, a corresponding equivalent risk neutral probability measure may, in general, not exist. Therefore, the derivation of risk neutral transition densities may not be that useful.

To illustrate the statement of Lemma 12.3.1, Fig. 12.3.2 displays a transition density of the GOP as a function of K and T, which has been numerically computed by application of relation (12.3.27). As input we used the values of the European call options that were calculated earlier under the modified CEV model for obtaining the implied volatilities shown in Fig. 12.2.3. This means that Fig. 12.3.2 displays an inferred real world transition probability density $p_{S^{\delta_*}}$ for a GOP process S^{δ_*} for the case of the modified CEV model with $a = -\frac{1}{2}$, $\psi = 0.2$ and $r = 0.04$.

Representation of the LV Function

We shall see under the LV model that, in principle, at any maturity date $T \in [0, \infty)$ and for any value $\kappa \in (0, \infty)$, the LV function value $\sigma(T, \kappa)$ can be recovered from a continuum of observed European call option prices. This is again similar to results described in Breeden & Litzenberger (1978), Dupire (1992, 1993, 1994) and Derman & Kani (1994a, 1994b). In our case the LV function is obtained without requiring the existence of an equivalent risk neutral probability measure, which is different to the approach taken in these references.

To derive the result conveniently let us make the following technical assumptions

$$\lim_{\kappa \to 0} \frac{1}{\kappa} \frac{\partial}{\partial T} u(t, \hat{S}_t^0, T, \kappa) = 0, \tag{12.3.28}$$

and

$$\lim_{\kappa \to 0} \sigma^2(T, K)\, \kappa\, \frac{\partial^2}{\partial \kappa^2} u(t, \hat{S}_t^0, T, \kappa) = 0. \tag{12.3.29}$$

These are reasonable conditions that apply to a wide range of LV models. They lead to the following result, which is derived in Heath & Platen (2006):

Theorem 12.3.2. *Under* (12.3.28) *and* (12.3.29) *has for fixed* $t \in [0, T]$ *and* $\hat{S}_t^0 > 0$ *the LV function the form*

$$\sigma(T, K) = \frac{\sqrt{2}}{\kappa} \left(\frac{\frac{\partial}{\partial T} u(t, \hat{S}_t^0, T, \kappa)}{\frac{\partial^2}{\partial \kappa^2} u(t, \hat{S}_t^0, T, \kappa)} \right)^{\frac{1}{2}} \tag{12.3.30}$$

for $(T, K) \in (0, \infty) \times (0, \infty)$, $t \in [0, T)$, *with* κ *as given in* (12.3.22).

Dupire Formula

To express the LV function in terms of European call option prices one can use the transformations (12.3.22) and (12.3.21) to compute the corresponding partial derivatives. One then obtains the following result, which is equivalent to (12.3.30), see Heath & Platen (2006). It is known as the *Dupire formula*. Here it is obtained without relying on the existence of a risk neutral probability measure.

Corollary 12.3.3. (Dupire) *The LV function has the representation*

$$\sigma(T, K) = \frac{\sqrt{2}}{K} \sqrt{\frac{\frac{\partial}{\partial T} c(t, S_t^{\delta_*}, T, K) + K\, r\, \frac{\partial}{\partial K} c(t, S_t^{\delta_*}, T, K)}{\frac{\partial^2}{\partial K^2} c(t, S_t^{\delta_*}, T, K)}} \tag{12.3.31}$$

for $(T, K) \in (0, \infty) \times (0, \infty)$, $t \in [0, T)$.

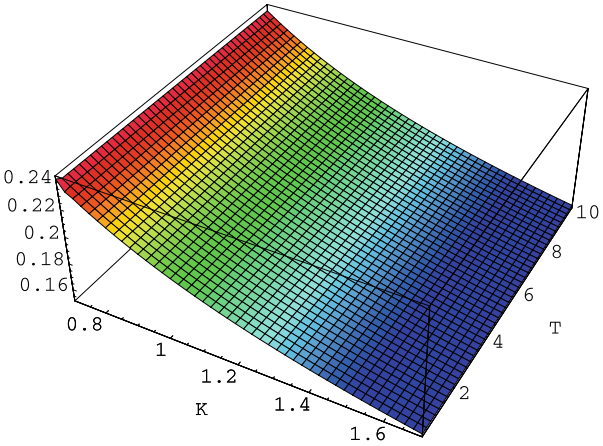

Fig. 12.3.3. LV function implied from modified CEV call option prices

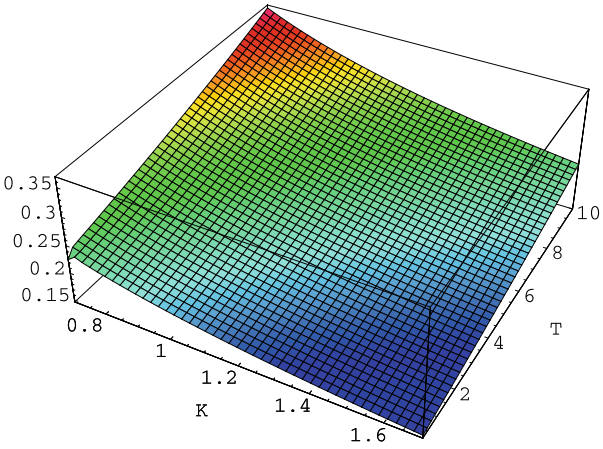

Fig. 12.3.4. LV function implied from MMM call option prices

For illustration, in Fig. 12.3.3 the LV function $\sigma(\cdot,\cdot)$ is displayed when obtained numerically via formula (12.3.31) from the European call option values that were used to compute the implied volatilities of the modified CEV model shown in Fig. 12.2.3. These results match, up to some negligible numerical errors, the corresponding LV function $\sigma(t,S) = S^{a-1}\psi$. Small errors in values are detectable in Fig. 12.3.3 for small K and T, which are caused by the numerical implementation of the formula (12.3.31). These minor differences are explained by round-off and truncation errors from the discrete differentiations involved. Similarly we plot in Fig. 12.3.4 the LV function, numerically implied from call prices under the stylized MMM. Also we recover here, up to minor numerical errors for small K and T, the LV function of the MMM.

It must be noted that a wide range of typically observed implied volatility surfaces can be calibrated via LV models. However, this does not mean that

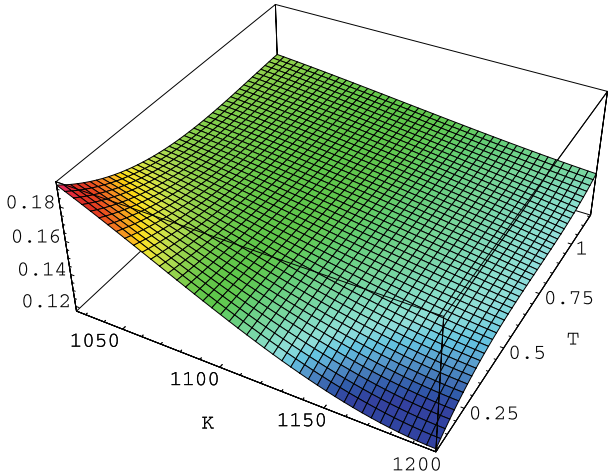

Fig. 12.3.5. Implied volatility surface for the S&P500 for 20 April 2004

the resulting LV model explains the dynamics of the underlying security. It only provides an LV function for European call and put options which allows us to match the observed option prices under the assumption of an LV model.

Finally, it is important to emphasize that implying a local volatility function from traded option prices is a difficult numerical task. Small deviations in prices can have a substantial effect on the implied LV function. This also creates a major drawback for the practical calibration of LV models. It would be valuable to have some economic reasoning behind the particular form of a selected LV function. The MMM, which we derive in the next chapter, provides such an economic explanation.

Local Volatility Function of S&P500

To illustrate the above analysis further we consider observed index option prices for the S&P500 index. Due to the numerical sensitivity of the implied LV functions to small errors in option prices we work with smoothed data. Figure 12.3.5 shows a fit of the implied volatility surface for S&P500 European call options for 20 April 2004 as in Heath & Platen (2006). These implied volatilities were computed using prices obtained from the average of bid and ask prices using the short rate $r = 0.03$ and a dividend rate of $d = 0.01$. The corresponding closing price for the S&P500 index was $S_0^{\delta_*} = 1114$. A total of 83 option prices was used to obtain the displayed fit. A least squares fit, see Sect. 2.3, for the implied volatility surface was obtained using a set of two-dimensional cubic polynomials. The corresponding smoothed option prices are then used to calculate the real world transition densities according to formula (12.3.27). The resulting transition density function is displayed in Fig. 12.3.6.

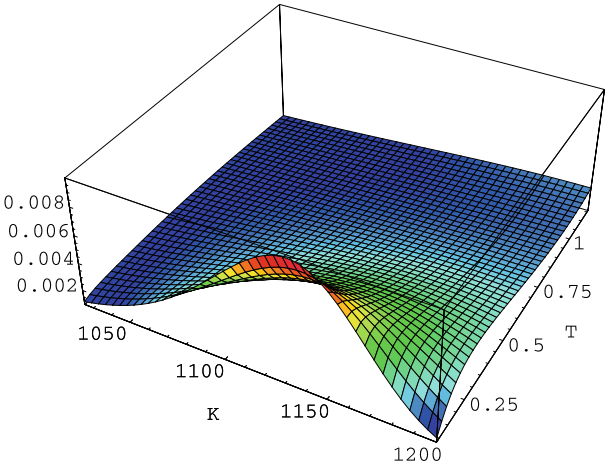

Fig. 12.3.6. Implied transition density for S&P500 for 20 April 2004

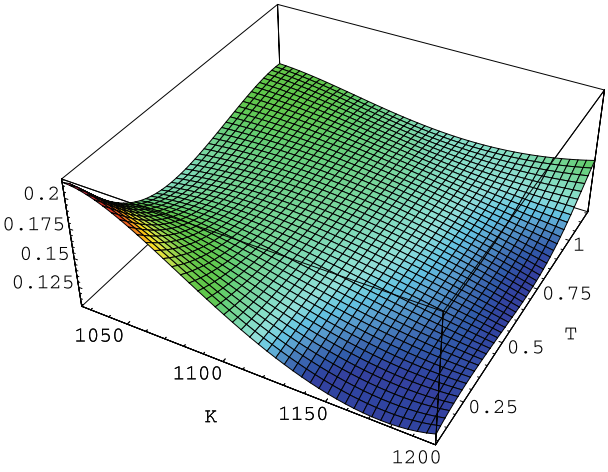

Fig. 12.3.7. LV function for S&P500 for 20 April 2004

The corresponding LV function is obtained by formula (12.3.31) and is displayed in Fig. 12.3.7. Because of the form of equation (12.3.31) and, in particular, the combination of first and second order partial derivatives, the shape of this surface turns out to be rather sensitive to the choice of the basis functions employed in the fitting procedure. Note that this LV function returns in our case exactly the implied volatility surface displayed in Fig. 12.3.5 and the corresponding smoothed S&P500 option prices. We observe a strong sensitivity of the LV function towards small deviations in option prices. Therefore, it is difficult to extract from observed data what the calibrated LV function of an index should be. The difficulties indicated above, in calibrating LV models in practice, emphasize the need for a better understanding of the nature of the volatility process itself. This should then provide a generic shape for the

LV function. In the next chapter we shall discuss this question further when deriving the MMM. It is interesting to note that the implied volatility surface in Fig. 12.3.5 is without any major curvature for times to maturity above six months. This is also the type of implied volatility surface that the MMM generates for this range of maturities, see Fig. 12.3.1.

Proof of Theorem 12.3.2 (*)

From the SDE (12.3.9) and relation (12.3.8) it follows that the transition density $p_{\hat{S}^0}$ for $\hat{S}^0$ satisfies the Fokker-Planck equation

$$\frac{\partial}{\partial T} p_{\hat{S}^0}(t, \hat{S}_t^0; T, \kappa) - \frac{1}{2} \frac{\partial^2}{\partial \kappa^2} \left\{ \sigma^2(T, K)\, \kappa^2\, p_{\hat{S}^0}(t, \hat{S}_t^0; T, \kappa) \right\} = 0 \tag{12.3.32}$$

for $(T, \kappa) \in (0, \infty) \times (0, \infty)$ with initial condition

$$p_{\hat{S}^0}(t, \hat{S}_t^0; t, \kappa) = \delta(\hat{S}_t^0 - \kappa), \tag{12.3.33}$$

where $\delta(\cdot)$ is the Dirac delta function, see (4.4.1). It, therefore, follows by using (12.3.25) that (12.3.32) can be rewritten in the form

$$\frac{\partial}{\partial T} \left(\frac{\partial^2}{\partial \kappa^2} u(t, \hat{S}_t^0, T, \kappa) \right) - \frac{1}{2} \frac{\partial^2}{\partial \kappa^2} \left\{ \sigma^2(T, K)\, \kappa^2\, \frac{\partial^2}{\partial \kappa^2} u(t, \hat{S}_t^0, T, \kappa) \right\} = 0$$

and hence

$$\frac{\partial^2}{\partial \kappa^2} \left\{ \frac{\partial}{\partial T} u(t, \hat{S}_t^0, T, \kappa) - \frac{1}{2} \sigma^2(T, K)\, \kappa^2\, \frac{\partial^2}{\partial \kappa^2} u(t, \hat{S}_t^0, T, \kappa) \right\} = 0. \tag{12.3.34}$$

Then there exist quantities $\beta_0(T)$ and $\beta_1(T)$ such that

$$\frac{\partial}{\partial T} u(t, \hat{S}_t^0, T, \kappa) - \frac{1}{2} \sigma^2(T, K)\, \kappa^2\, \frac{\partial^2}{\partial \kappa^2} u(t, \hat{S}_t^0, T, \kappa) = \beta_0(T) + \beta_1(T)\, \kappa. \tag{12.3.35}$$

From (12.3.35), (12.3.28) and (12.3.29) it follows that

$$\beta_0(T) = 0. \tag{12.3.36}$$

and

$$\beta_1(T) = 0. \tag{12.3.37}$$

Combining (12.3.35), (12.3.36) and (12.3.37) yields (12.3.30). □

12.4 Stochastic Volatility Models

Modeling Volatility as a Separate Process

A number of continuous asset price models have been developed, which model the volatility process as a separate, possibly correlated, stochastic process.

This group of models includes the models by Hull & White (1987, 1988), Johnson & Shanno (1987), Scott (1987), Wiggins (1987), Chesney & Scott (1989), Melino & Turnbull (1990), Stein & Stein (1991), Hofmann et al. (1992) and Heston (1993) among others. In the following we provide a description of this type of model by applying results from Heath, Hurst & Platen (2001). The GOP models again an index which is interpreted as the underlying security.

The empirical results of Sect. 2.6 on the estimation of index log-returns indicate that for daily observations of stock index log-returns the Student t distribution with about four degrees of freedom provides an excellent fit. We take this stylized empirical fact as motivation for the following study, which aims to construct stochastic volatility processes with a prescribed stationary density.

First, let us explain how this is linked to the results from the estimation of prescribed log-return densities. When considering small time steps, then a discounted GOP $\bar{S}^{\delta_*}$ with squared volatility $|\theta_t|^2$ generates at time t approximately conditionally Gaussian distributed log-returns with a stochastic variance $|\theta_t|^2$ per unit of time. This means that for small time step size $h > 0$ one observes the conditionally Gaussian log-returns

$$\Delta \ln(\bar{S}_t^{\delta_*}) = \ln\left(\frac{\bar{S}_{t+h}^{\delta_*}}{\bar{S}_t^{\delta_*}}\right) \sim \mathcal{N}\left(\frac{|\theta_t|^2}{2}\, h, |\theta_t|^2\, h\right). \tag{12.4.1}$$

Since we consider log-returns over a short time period $[t, t+h]$ the trend effect of the conditional mean in (12.4.1) can be neglected.

We now consider the case where the process $|\theta|^2$ has a given stationary density and the observation of the log-returns extends over a sufficiently long time period. This then results in the estimation of normal variance mixture log-returns, as described in Sect. 2.5, see also Fergusson & Platen (2006). For instance, when $\frac{1}{|\theta_t|^2}$ has as stationary density that of a gamma distributed random variable, then the estimated log-returns appear to be Student t distributed, see Kessler (1997) and Prakasa Rao (1999). On the other hand, if the stationary density of $|\theta_t|^2$ is a gamma density, then the log-returns, when estimated, appear to be variance gamma distributed. We emphasize the fact that a stochastic volatility process needs a long observation period so that the squared volatility values have traversed reasonably often over the range of their typical values to generate the mixing effect of the random variance for the log-returns.

A Class of Continuous Stochastic Volatility Models

Note from (12.1.1) that the discounted GOP

$$\bar{S}_t^{\delta_*} = \frac{S_t^{\delta_*}}{S_t^0} \tag{12.4.2}$$

satisfies the SDE

$$d\bar{S}_t^{\delta_*} = \bar{S}_t^{\delta_*} \left(|\theta_t|^2 \, dt + |\theta_t| \, dW_t \right) \tag{12.4.3}$$

for $t \in [0, \infty)$. Similarly to Heath, Hurst & Platen (2001) we now derive a class of continuous discounted GOP models with stochastic volatility processes that have stationary densities. To cover a wide range of stochastic volatility models let us consider the factor process $X = \{X_t, \, t \in [0, \infty)\}$ with

$$X_t = Y(|\theta_t|). \tag{12.4.4}$$

It involves a twice continuously differentiable function $Y(\cdot)$ that depends on the volatility process $|\theta| = \{|\theta_t|, \, t \in [0, \infty)\}$ of the GOP. The joint dynamics of the discounted GOP process $\bar{S}^{\delta_*}$ and the factor process X are assumed to be governed by a time homogeneous system of SDEs

$$\begin{aligned} d\bar{S}_t^{\delta_*} &= \bar{S}_t^{\delta_*} \left(|\theta_t|^2 \, dt + |\theta_t| \left(\varrho \, d\bar{W}_t + \sqrt{1 - \varrho^2} \, d\tilde{W}_t \right) \right), \\ dX_t &= C(X_t) \, dt + D(X_t) \, d\bar{W}_t \end{aligned} \tag{12.4.5}$$

for $t \in [0, \infty)$. Here $\tilde{W}$ and $\bar{W}$ are independent standard Wiener processes under the real world probability measure P. In the SDE (12.4.5) the dynamics of the discounted GOP $\bar{S}^{\delta_*}$ involve the stochastic volatility process $|\theta|$. The functions $C(\cdot)$ and $D(\cdot)$ are assumed to satisfy appropriate conditions so that the SDE (12.4.5) admits a unique strong solution, see Sect. 7.7. The parameter $\varrho \in [-1, 1]$ is the correlation parameter.

We remark that, by application of the Itô formula to the function (12.4.4) of $X_t = Y(|\theta_t|)$, we obtain the SDE

$$dX_t = dY(|\theta_t|) = Y'(|\theta_t|) \, d|\theta_t| + \frac{1}{2} Y''(|\theta_t|) \, d[|\theta|]_t$$

and, thus, by rearranging this SDE for $d|\theta_t|$ with (12.4.5) the SDE

$$d|\theta_t| = \frac{1}{Y'(|\theta_t|)} \left(C(X_t) \, dt - \frac{1}{2} Y''(|\theta_t|) \, d[|\theta|]_t + D(X_t) \, d\bar{W}_t \right).$$

This leads to an SDE for the volatility process $|\theta| = \{|\theta_t| = Y^{-1}(X_t), \, t \in [0, \infty)\}$, which is of the form

$$d|\theta_t| = \left(\frac{C(Y(|\theta_t|))}{Y'(|\theta_t|)} - \frac{1}{2} \frac{D(Y(|\theta_t|))^2 \, Y''(|\theta_t|)}{Y'(|\theta_t|)^3} \right) dt + \frac{D(Y(|\theta_t|))}{Y'(|\theta_t|)} \, d\bar{W}_t \tag{12.4.6}$$

for $t \in [0, \infty)$. Here $Y'(\cdot)$ and $Y''(\cdot)$ denote the first and second derivatives of the function $Y(\cdot)$, respectively, and $Y^{-1}(\cdot)$ is the inverse function of $Y(\cdot)$ on $(0, \infty)$. The resulting stochastic volatility models differ according to different specifications of the functions $Y(\cdot)$, $C(\cdot)$ and $D(\cdot)$.

Specific Stochastic Volatility Models

Let us now mention some well-known stochastic volatility models and explain how they fit into the above framework:

Hull & White (1988) proposed a model with mean reverting dynamics for the squared volatility process $|\theta|^2$. Here $X_t = Y(|\theta_t|) = |\theta_t|^2$, $C(x) = k\,(\bar{\theta}^2 - x)$ and $D(x) = \gamma\,\sqrt{x}$, where k, $\bar{\theta}$ and γ are positive constants. This is also the dynamics used in Heston (1993). It provides a popular squared stochastic volatility model, the *Heston model*, which satisfies the SDE

$$d|\theta_t|^2 = k\,(\bar{\theta}^2 - |\theta_t|^2)\,dt + \gamma\,\sqrt{|\theta_t|^2}\,d\bar{W}_t \tag{12.4.7}$$

for $t \in [0, \infty)$ with $|\theta_0|^2 > 0$. Note that one needs to have $\frac{\kappa}{\gamma^2} \geq \frac{1}{2}$ to obtain a stationary density for the stochastic volatility since the squared volatility is modeled by a square root process, see Sect. 8.7.

Scott (1987) and Stein & Stein (1991) used Ornstein-Uhlenbeck processes to model the volatility process $|\theta|$, where $X_t = Y(|\theta_t|) = |\theta_t|$, $C(x) = k\,(\bar{\theta} - x)$ and $D(x) = \gamma$. Here k, $\bar{\theta}$ and γ are positive constants. The *Scott model* is defined by the SDE

$$d|\theta_t| = k\,(\bar{\theta} - |\theta_t|)\,dt + \gamma\,d\bar{W}_t \tag{12.4.8}$$

for $t \in [0, \infty)$, $|\theta_0| \in \Re$. Note that the squared volatility $|\theta_t|^2$ satisfies the SDE

$$d|\theta_t|^2 = 2\,k\left(\bar{\theta}\,|\theta_t| + \frac{\gamma^2}{2\,k} - |\theta_t|^2\right)dt + 2\,\gamma\,|\theta_t|\,d\bar{W}_t, \tag{12.4.9}$$

which resembles some generalized square root process.

Also Wiggins (1987), Chesney & Scott (1989) and Melino & Turnbull (1990) used the Ornstein-Uhlenbeck process, but for modeling the logarithm $\ln(|\theta_t|)$ of the volatility process. Here $X_t = Y(|\theta_t|) = \ln(|\theta_t|)$, $C(x) = k(\ln(\bar{\theta}) - x)$ and $D(x) = \gamma$, where, once again, k, $\bar{\theta}$ and γ are positive constants. The *Wiggins model* satisfies then the SDE

$$d\ln(|\theta_t|) = k\left(\ln(\bar{\theta}) - \ln(|\theta_t|)\right)dt + \gamma\,d\bar{W}_t \tag{12.4.10}$$

for $t \in [0, \infty)$, $|\theta_0| > 0$. The squared volatility satisfies here the SDE

$$d|\theta_t|^2 = |\theta_t|^2\left(2\,\gamma^2 + k\,(\ln(\bar{\theta}^2) - \ln(|\theta_t|^2))\right)dt + 2\,\gamma\,|\theta_t|^2\,d\bar{W}_t, \tag{12.4.11}$$

which has multiplicative noise. Note that further stochastic volatility models can be expressed under the above framework, as we shall see below.

Stationary Density

Let us now compute the stationary density for the process X given by the SDE (12.4.5). The process X is a time homogeneous diffusion process with

transition densities depending only on the elapsed period of time. We, therefore, write $p(s,x;t,y)$ to denote the transition density of $X_t = y$ given $X_s = x$. The corresponding *Fokker-Planck equation*, see (4.4.1), is then given by

$$\frac{\partial p(s,x;t,y)}{\partial t} + \frac{\partial (C(y)\, p(s,x;t,y))}{\partial y} - \frac{1}{2}\, \frac{\partial^2 \left(D(y)^2\, p(s,x;t,y)\right)}{\partial y^2} = 0 \quad (12.4.12)$$

for all $t \in (s,\infty)$ and $s \in [0,\infty)$, with (s,x) fixed.

Since X is assumed to have a stationary density the transition density $p(s,x;t,y)$ approaches the stationary density function $\bar{p}$ as $t \to \infty$, that is

$$\bar{p}(y) = \lim_{t\to\infty} p(0,x;t,y), \quad (12.4.13)$$

for $x, y \in \Re$. It follows by the Fokker-Planck equation (12.4.12) that

$$C(y)\bar{p}(y) - \frac{1}{2}\frac{d(D(y)^2\, \bar{p}(y))}{dy} = \tilde{K}, \quad (12.4.14)$$

for all $y \in \Re$ and some constant $\tilde{K}$. Now, we assume that $\bar{p}(y) \to 0$ and $\frac{d\bar{p}(y)}{dy} \to 0$ as $|y| \to \infty$. Under these assumptions the constant $\tilde{K}$ must become zero. By direct integration we then obtain, as shown in (4.5.5),

$$\bar{p}(y) = \frac{A}{D(y)^2}\, \exp\left\{2 \int_{y_0}^{y} \frac{C(u)}{D(u)^2}\, du\right\} \quad (12.4.15)$$

for $y \in \Re$, where A is a normalizing constant such that

$$\int_{-\infty}^{\infty} \bar{p}(y)\, dy = 1.$$

Here y_0 is an appropriately chosen point in $(-\infty,\infty)$. Note that (12.4.15) gives the form of the stationary density function and accommodates a wide range of diffusions X with stationary density.

Inverse Gamma Density

As pointed out in Sect. 2.6, we obtain the Student t distribution as normal variance mixture log-return distribution if the squared volatility has an inverse gamma distribution. Therefore, let us now introduce a class of squared volatility models, which have for

$$X_t = |\theta_t|^2 \quad (12.4.16)$$

an inverse gamma density as stationary density. As we shall see below, several diffusion processes can fulfill this requirement. The stationary density $\bar{p}_{\theta^2}$ for the squared volatility equals in this case

$$\bar{p}_{\theta^2}(y) = \frac{(\frac{1}{2}\,\delta)^{\frac{1}{2}\,\delta}}{\varepsilon^2\,\Gamma(\frac{1}{2}\,\delta)}\,\left(\frac{y}{\varepsilon^2}\right)^{-\frac{1}{2}\,\delta-1}\,\exp\left\{-\frac{\frac{1}{2}\,\delta\,\varepsilon^2}{y}\right\}, \tag{12.4.17}$$

for $y > 0$ with $\delta > 0$ degrees of freedom and scaling parameter ε, where $\Gamma(\cdot)$ denotes the gamma function, see (1.2.10). Note that we model here the density of the *inverse* of a random variable that is gamma distributed.

After rearrangement of (12.4.14) we obtain the formula

$$C(x) = \frac{1}{2\,\bar{p}_{\theta^2}(x)}\,\frac{d(D(x)^2\bar{p}_{\theta^2}(x))}{dx}, \tag{12.4.18}$$

for $x > 0$. The function $C(\cdot)$ is therefore solely determined by the probability density function $\bar{p}_{\theta^2}(\cdot)$ for the stationary density of $|\theta|^2$ and the function $D(\cdot)$.

To be specific and obtain still a rich class of diffusions X we let the diffusion coefficient function $D(\cdot)$ of X have the form of a power function

$$D(x) = \gamma\,x^{\xi}, \tag{12.4.19}$$

for $x > 0$ with some positive constants γ and ξ. This particular choice for the functional form of $D(\cdot)$ ensures that the diffusion coefficient of the squared volatility approaches zero when the squared volatility approaches zero. Furthermore, the exponent ξ controls the feedback of the squared volatility on its diffusion coefficient. With this functional form for $D(\cdot)$ and the probability density function $\bar{p}_{\theta^2}$ in (12.4.17), the equation (12.4.18) provides for the squared volatility process X the drift function

$$C(x) = k\,x^{2(\xi-1)}\,(\bar{\theta}^2 - x), \tag{12.4.20}$$

for $x > 0$, where $k = \frac{1}{4}\,\gamma^2\,(\delta + 2 - 4\,\xi)$, $\bar{\theta}^2 = \frac{\varepsilon^2\,\delta}{\delta+2-4\,\xi}$ and $\delta > 4\,\xi - 2$. In the special case $\delta + 2 - 4\xi = 0$ we set $k\bar{\theta}^2 = \frac{\gamma^2\varepsilon^2\delta}{4}$. The resulting family of discounted GOP models is, therefore, characterized by a squared volatility with SDE

$$d|\theta_t|^2 = k\,|\theta_t|^{4(\xi-1)}\,(\bar{\theta}^2 - |\theta_t|^2)\,dt + \gamma\,|\theta_t|^{2\,\xi}\,d\bar{W}_t, \tag{12.4.21}$$

where $k, \bar{\theta}, \gamma$ and ξ are all constants. Note that for a desired degree of freedom δ for the inverse gamma density (12.4.17) the parameters k, ξ, γ and $\bar{\theta}^2$ cannot be chosen freely. In particular, we need to set

$$\delta = \frac{2\,(2\,\xi - 1)}{1 - \frac{\varepsilon^2}{\bar{\theta}^2}}. \tag{12.4.22}$$

It is important to note that several existing models are included in this class of squared volatility models. For the choice of the exponent $\xi = 1$ we obtain the *ARCH diffusion model*

$$d|\theta_t|^2 = k\,(\bar{\theta}^2 - |\theta_t|^2)\,dt + \gamma\,|\theta_t|^2\,d\bar{W}_t, \tag{12.4.23}$$

which is the continuous time limit of the innovation process of the GARCH(1,1) and NGARCH(1,1) models described in Nelson (1990) and Frey (1997). The class of ARCH and GARCH time series models, which have many generalizations, was originally developed in Engle (1982). When taking the continuous time limit in a GARCH(1,1) model, see Nelson (1990), the underlying security and the squared volatility process appear to be driven by independent Wiener processes. The leverage effect, see Sect. 12.1, can be modeled in (12.4.23) when $\bar{W}$ and W are assumed to be negatively correlated.

When the exponent is set to $\xi = \frac{3}{2}$ and $\varrho = -1$ we obtain the 3/2 *model*

$$d|\theta_t|^2 = k\,|\theta_t|^2\,(\bar{\theta}^2 - |\theta_t|^2)\,dt + \gamma\,(|\theta_t|^2)^{\frac{3}{2}}\,d\bar{W}_t. \tag{12.4.24}$$

It corresponds to the squared volatility model suggested in Platen (1997) and covers the volatility structure of the *stylized MMM* mentioned in Sect. 7.5, see Platen (2001, 2002). We remark that in Lewis (2000) a version of a 3/2 model was studied among other models.

ARCH Diffusion Model

Let us now investigate effects generated by the ARCH diffusion model considered in Hurst (1997), Lewis (2000) and Heath, Hurst & Platen (2001). This means, we consider the case $\xi = 1$ in (12.4.21).

In the following, the speed of adjustment is chosen to be $k = 2.0$ so that the half-life time of shocks, $\frac{\ln(2)}{k}$, is approximately eighteen weeks. The volatility of the squared volatility is set to $\gamma = 1.0$ so that the volatility of volatility is approximately 0.5. These choices for k and γ ensure a strong stochastic volatility effect. The initial squared volatility $|\theta_0|^2$ and the long term mean of the squared volatility $\bar{\theta}^2$ are both chosen to equal 0.04 so that initial and long term volatility are approximately 0.2. Furthermore, the correlation ϱ is, for simplicity, first set to zero. The initial discounted GOP value is set to $\bar{S}_0^{\delta_*} = 100$ with a short rate of $r = 0.04$. The effect of changing each of these parameters, while keeping the others constant, is examined below.

Figure 12.4.1 displays the implied volatility surface for European call options with maturity dates, ranging from five weeks to one year and the strike K ranging from 80 to 125. These kind of implied volatility surfaces are often observed for currency and equity options but not for index options. Note that the magnitude of the implied volatility smile or curvature decreases as the time to maturity increases. The smile effect for short dated options is very prominent but becomes less pronounced for longer dated options.

The effect of changing the correlation ϱ on the implied volatility surface is now examined. Figure 12.4.2 shows implied volatilities for European call options with correlation ϱ ranging from -0.5 to 0.5 and the strike K ranging from 80 to 125, where the time to maturity is six months. When the correlation is negative it can be seen that out-of-the-money options have lower implied

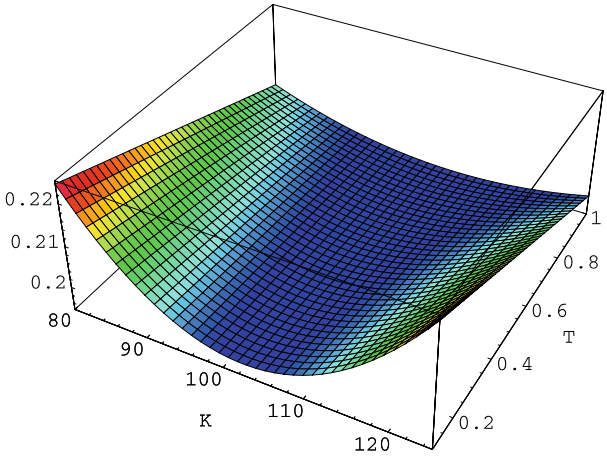

Fig. 12.4.1. Implied volatility surface for zero correlation

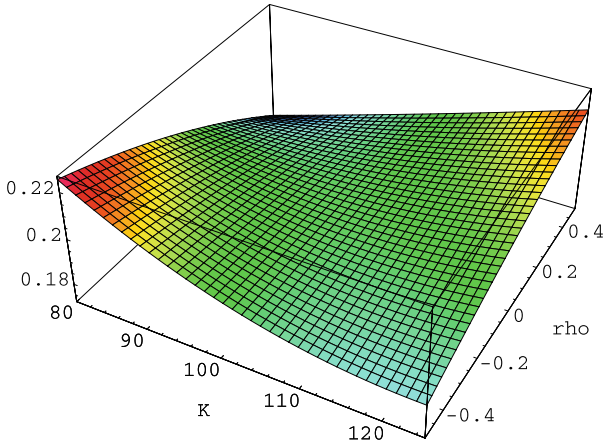

Fig. 12.4.2. Effect of changing correlation on implied volatilities

volatilities than in-the-money options. This effect is commonly called a negative implied volatility skew. Usually, for index options the implied volatilities are negatively skewed, see Fig. 12.1.5, reflecting the leverage effect created by negatively correlated index and volatility increments. Thus, with the choice $\varrho < 0$ the typical implied volatility curves for indices can be generated. Note that for $\varrho > 0$ a strong positively skewed implied volatility curve can be obtained.

Figure 12.4.3 displays implied volatilities for European call options with the speed of adjustment parameter k ranging from 1 to 20, the strike K ranging from 80 to 125 and where the time to maturity is six months. It can be observed that as the speed of adjustment parameter k increases, the magnitude of the implied volatility smile decreases.

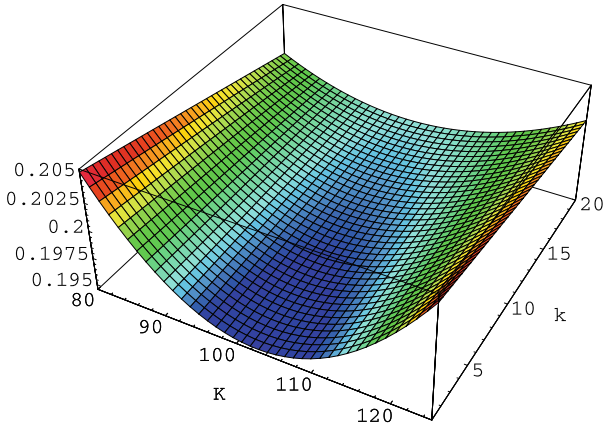

Fig. 12.4.3. Effect of changing speed of adjustment on implied volatilities

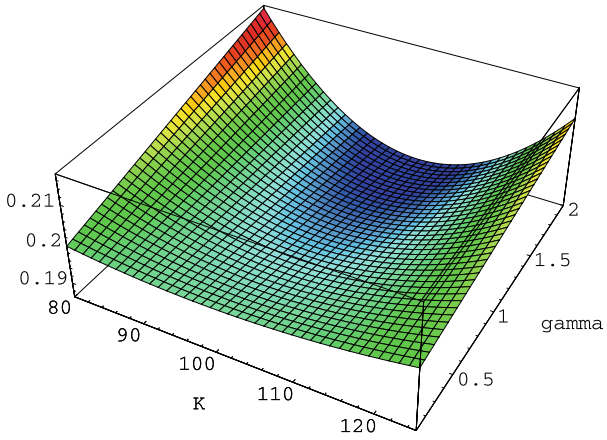

Fig. 12.4.4. Effect of changing volatility of the squared volatility on implied volatilities

Figure 12.4.4 depicts implied volatilities for European call options with the volatility γ of squared volatility ranging from 0.1 to 2, or volatility of volatility ranging from approximately 0.5 to 1, the strike K ranging from 80 to 125 and where the time to maturity is six months. Note that, as the volatility of squared volatility increases, the magnitude of the implied volatility smile increases. For $\gamma = 0$ we have a version of the BS model with no deformation or curvature in the implied volatility surface.

It is apparent that the ARCH diffusion model in (12.4.23) captures some of the typical properties of implied volatilities observed in index option markets, see Fig. 12.1.5. However, to generate such a negatively skewed implied volatility surface one needs to consider a rather strong negative correlation parameter $\varrho < 0$. As is evident from Fig. 12.4.2, the ARCH diffusion model with strong negative correlation can generate the negative skew pattern. Therefore,

it can model some leverage effect. However, it requires a separate stochastic volatility process to achieve this. Other stochastic volatility models produce similar results to what has been demonstrated above for the ARCH diffusion model, see, for instance, Cont & Tankov (2004) and results on the MMM in the next chapter. This makes it difficult to decide which is potentially a better model.

An important drawback of the above stochastic volatility models is that they are genuine two-factor models, driven by two separate stochastic processes. This makes it a complex numerical task to value even standard index derivatives. A parsimonious, economically based one-factor model, which can generate similar skews and smiles in implied volatility surfaces, would be preferable. In particular, if it could explain the nature of the dynamics of the underlying index.

12.5 Exercises for Chapter 12

12.1. Prove that the ARCH diffusion model for squared volatility

$$d|\theta_t|^2 = \kappa\,(\bar{\theta}^2 - |\theta_t|^2)\,dt + \gamma\,|\theta_t|^2\,dW_t$$

has an inverse gamma density as stationary density.

12.2. Show that the squared volatility of the model

$$d|\theta_t|^2 = \kappa\,|\theta_t|^2\,(\bar{\theta}^2 - |\theta_t|^2)\,dt + \gamma\,|\theta_t|^3\,dW_t$$

has an inverse gamma density.

12.3. Compute the stationary density for the squared volatility for the Heston model

$$d|\theta_t|^2 = \kappa\,(\bar{\theta}^2 - |\theta_t|^2)\,dt + \gamma\,||\theta_t||\,dW_t.$$

12.4. Calculate the stationary density for the squared volatility $|\theta_t|^2$ of the Scott model, where

$$d|\theta_t| = \kappa\,(\bar{\theta} - |\theta_t|)\,dt + \gamma\,dW_t.$$

Characterize the type of the stationary density ?

12.5. Calculate the stationary density for the squared volatility $|\theta_t|^2$, which satisfies the SDE

$$d\ln(|\theta_t|^2) = \kappa\,(\bar{\xi} - |\theta_t|^2)\,dt + \gamma\,dW_t.$$

Which type of density is this ?

12.6. (*) Show under the modified CEV model that the benchmarked savings account and, thus, the benchmarked savings bond are strict local martingales.